Biogeosciences, 22, 1393–1411, 2025
https://doi.org/10.5194/bg-22-1393-2025

Biogeosciences
Open Access
Research article

Impact of winter warming on CO_2 fluxes in evergreen needleleaf forests

Mana Gharun[1], Ankit Shekhar[2,11], Lukas Hörtnagl[2], Luana Krebs[2], Nicola Arriga[3], Mirco Migliavacca[3], Marilyn Roland[4], Bert Gielen[4], Leonardo Montagnani[5], Enrico Tomelleri[5], Ladislav Šigut[6], Matthias Peichl[7], Peng Zhao[7], Marius Schmidt[8], Thomas Grünwald[9], Mika Korkiakoski[10], Annalea Lohila[10], and Nina Buchmann[2]

[1]Institute of Landscape Ecology, University of Münster, 48149 Münster, Germany
[2]Department of Environmental Systems Science, Institute of Agricultural Sciences, ETH Zurich, Zurich, Switzerland
[3]European Commission, Joint Research Centre (JRC), Ispra, Italy
[4]Plants and Ecosystems (PLECO), Department of Biology, University of Antwerp, 2610 Wilrijk, Belgium
[5]Faculty of Agricultural, Environmental and Food Sciences, Free University of Bozen-Bolzano, Faculty of Agricultural, Environmental and Food Sciences, 39100 Bolzano, Italy
[6]Global Change Research Institute, Czech Academy of Sciences (CAS), Bělidla 986/4a, 60300 Brno, Czech Republic
[7]Department of Forest Ecology and Management, Swedish University of Agricultural Sciences (SLU), 901 83 Umeå, Sweden
[8]Institute for Bio-and Geosciences (IBG), Agrosphere (IBG-3), Institute of Bio- and Geosciences, Forschungszentrum Jülich, 52425 Jülich, Germany
[9]Department of Hydro Sciences, Institute of Hydrology and Meteorology, Technical University of Dresden, 01062 Dresden, Germany
[10]Finnish Meteorological Institute, Climate System Research, Helsinki, Finland
[11]Agricultural and Food Engineering Department, Indian Institute of Technology Kharagpur, Kharagpur, India

Correspondence: Mana Gharun (mana.gharun@wwu.de)

Received: 8 December 2023 – Discussion started: 4 January 2024
Revised: 17 December 2024 – Accepted: 19 December 2024 – Published: 12 March 2025

Abstract. Compared to drought and heat waves, the impact of winter warming on forest CO_2 fluxes has been less studied, despite its significant relevance in colder regions with higher soil carbon content. Our objective was to test the effect of the exceptionally warm winter of 2020 on the winter CO_2 budget of cold-adapted evergreen needleleaf forests across Europe and identify the contribution of climate factors to changes in winter CO_2 fluxes. Our hypothesis was that warming in winter leads to higher emissions across colder sites due to increased ecosystem respiration. To test this hypothesis, we used 98 site-year eddy covariance measurements across 14 evergreen needleleaf forests (ENFs) distributed from the north to the south of Europe (from Sweden to Italy). We used a data-driven approach to quantify the effect of radiation, air temperature, and soil temperature on changes in CO_2 fluxes during the warm winter of 2020. Our results showed that warming in winter decreased forest net ecosystem productivity (NEP) significantly across most sites. The contribution of climate variables to CO_2 fluxes varied across the sites: in southern regions with warmer mean temperatures, radiation had a greater influence on NEP. Conversely, at colder sites, air temperature played a more critical role in affecting NEP. During the warm winter of 2020, colder regions experienced larger air temperature anomalies compared to the other sites; however we did not observe a significantly larger increase at colder sites due to winter warming. The varying responses of NEP across different sites highlight the complex interactions between climate variables such as air temperature, soil temperature, and radiation. These findings underscore the importance of integrating winter warming effects to more accurately predict the impacts of climate change on forest carbon dynamics.

1 Introduction

One of the key challenges in assessing the role of forests in mitigating climate change lies in understanding how forest CO_2 fluxes respond to extreme climatic conditions, particularly increases in air temperature. While forests serve as a significant sink for anthropogenic CO_2 emissions (Friedlingstein et al., 2023), extreme warming events can compromise their ability to sequester carbon effectively (Shekhar et al., 2023; Gharun et al., 2024). Although much research has focused on extreme events during the growing season, the impacts of warming winters remain relatively understudied (Kreyling et al., 2019).

In regions where evergreen conifers predominate, such as northern latitudes or higher altitudes, winter warming events can be particularly pronounced (IPCC, 2014). For instance, in 2020, Europe witnessed its warmest winter on record since 1981, with the most significant deviation from the reference period (1981–2020) observed in northeastern Europe (Copernicus Climate Change Service (C3S), 2020). However, the specific effects of such winter warming on CO_2 fluxes, especially in forested areas covered by snow and rich in soil carbon content, remain unclear.

1.1 Effect of warming on forest carbon fluxes

Forest net ecosystem productivity (NEP) depends on the balance between gross ecosystem CO_2 uptake (gross primary productivity, GPP) and emission (ecosystem respiration, R_{eco}). Both of these flux components are highly sensitive to climate drivers (e.g., air temperature, soil temperature, solar radiation). When canopy structural changes from one year to another are negligible, the interannual variations can be predominantly explained by changes in the climatic conditions (Hui et al., 2003). Net ecosystem productivity can increase or decrease with changes in temperature (Shekhar et al., 2023). In temperature-limited ecosystems for example, an increase in air temperature increases photosynthesis, which leads to higher gross productivity and potentially increased net CO_2 uptake (if respiration does not increase more) (Lin et al., 2021). However with warming and increased temperatures, respiration (autotrophic and heterotrophic) can also increase, and the balance of this with changes in gross productivity could lead to an increase, no change, or a reduction in net CO_2 uptake (Gharun et al., 2020).

Evergreen forests in the Northern Hemisphere contribute significantly to terrestrial carbon (C) storage and exchange (Beer et al., 2010; Thurner et al., 2014). High-latitude evergreen forests have shown an increase in gross primary productivity (GPP) with increasing temperature largely due to longer growing seasons (Myneni et al., 1997; Randerson et al., 1999; Forkel et al., 2016). Multiple other changes under warming however could counteract such an increase for the overall CO_2 uptake capacity of the forest (e.g., due to an increase in ecosystem respiration). In the absence of soil moisture limitation, respiration increases exponentially with an increase in temperature (Law et al., 1999). Additionally, in the presence of winter warming, despite more favorable conditions for photosynthesis, factors such as water stress or photoinhibition caused by high photon flux densities, in combination with low air temperatures, could downregulate photochemical efficiency and negatively affect net photosynthesis, which could reduce gross primary productivity (Troeng and Linder, 1982).

The temperature sensitivity of ecosystem respiration regulates how the terrestrial CO_2 emissions respond to a warming climate. Within naturally occurring temperature ranges, ecosystem respiration (sum of autotrophic and heterotrophic respirations) typically shows an exponential increase with temperature (Lloyd and Taylor, 1994). Previous studies, such as Chen et al. (2020), have demonstrated that Q_{10}, which reflects the rate of increase in soil respiration with a 10 °C rise in temperature, tends to increase as site mean temperatures decrease. However, the temperature sensitivity of ecosystem respiration is influenced not only by the direct effects of temperature on metabolic activity in plants and microorganisms but also by indirect factors such as moisture levels, the leaf area index, photosynthate input, litter quality, and microbial community composition. For example soil moisture affects the microbial activity and decomposition rates, which in turn influence respiration rates. In moist conditions, microbial activity increases, leading to increased decomposition and respiration rates. Conversely, in dry conditions, microbial activity slows down, reducing the respiration rates. The amount of organic matter produced through photosynthesis affects the availability of substrates for microbial decomposition, and higher photosynthate input results in increased carbon availability, stimulating microbial activity and respiration rates (Reichstein et al., 2002; Fierer et al., 2005; Lindroth et al., 2008; Migliavacca et al., 2011; Karhu et al., 2014; Collalti et al., 2020). The temperature response of net ecosystem productivity is the product of the sensitivity of GPP and ecosystem respiration to temperature (Lloyd and Taylor, 1994; Niu et al., 2011), and the temperature sensitivity of respiration (Q_{10}) changes proportionally with the site mean temperature (e.g., higher Q_{10} at colder sites; Chen et al., 2020).

In forests, the tree canopy serves as a thermal buffer, moderating the microclimatic below by insulating sub-canopy air. This leads to notable differences between sub-canopy and open-air temperatures, with sub-canopy air temperatures averaging 2 °C higher during winter months (Haesen et al., 2021). Teasing apart the effect of soil versus air temperature on fluxes is important firstly because soil and air temperatures can diverge by as much as 10 °C (Lembrechts et al., 2022) and secondly because air temperature and soil temperature affect CO_2 fluxes differently. Warming of the air increases leaf temperature, predominantly affecting the photosynthetic process in the leaves and CO_2 uptake, while soil temperature more directly influences root and microbial activity and thus influences soil respiration and CO_2 release (Berry and Björkman, 1980; Lloyd and Taylor, 1994).

1.2 Importance of the winter period for evergreen needleleaf forests (ENFs)

Environmental cues such as temperature, photoperiod, and light quality control a network of signalling pathways that coordinate cold acclimation and cold hardiness in trees that ensure survival during long periods of low temperature and freezing (Öquist and Huner, 2003; Ensminger et al., 2006). These signalling pathways include the gating of cold responses by the circadian clock, the interaction of light quality and photoperiod, and the involvement of phytohormones in low-temperature acclimation (Chang et al., 2021). Soluble carbohydrates, including sucrose (most abundant), accumulate in response to low temperatures, starting in late autumn and continuing throughout winter (Strimbeck and Schaberg, 2009; Chang et al., 2015). Persistent uninterrupted cold periods thus play an important role in forming the photosynthetic capacity of the trees as warmer winter temperatures increase the chance of photo-oxidative frost damage during earlier stages of the growing season (Gu et al., 2008; Chamberlain et al., 2019) which would compromise the forest's capacity for CO_2 uptake throughout the year (Desai et al., 2016). The risk of photo-oxidative frost damage increases with winter warming, as warmer winter temperatures can lead to an accumulation of photosynthetically active compounds in plants, and when sudden frost events occur during periods of high radiation, the combination of low temperatures and intense sunlight can induce photo-oxidative stress in plant tissues. This occurs because the photosynthetic machinery is still active but the low temperatures impair the plant's ability to dissipate excess energy, leading to the production (and imbalance) of reactive oxygen species (ROSs) that can damage cells and tissues. Photochemical damage can also happen in the case of high radiation, low water content in the leaf tissue, and low temperature, when photosynthesis and protein turnover become inhibited by low temperatures and when non-photochemical, heat dissipation mechanisms are insufficient to deal with excess excitation (hence the negative effect of freezing temperatures after dehardening) (Öquist and Huner, 2003).

Experimental evidence from temperature-sensitive conifers shows that warm spells in winter can induce premature dehardening of buds and result in stunted shoot development in the following spring (Nørgaard Nielsen and Rasmussen, 2008). Additionally, increased respiration due to warming can deplete stored non-structural carbohydrates (NSCs) and tree hydraulic functioning (if combined with drought) and affect tree functioning in spring (Sperling et al., 2015).

The winter of 2019–2020 was reported as the hottest winter in the last 4 decades (1981–2022) across Europe (Copernicus Climate Change Service, ECMWF). When compared to the average conditions, up to 45 fewer winter ice days were detected in eastern Europe and Russia (Copernicus Climate Change Service, Koninklijk Nederlands Meteorologisch Instituut (KNMI)). In Finland, for example, the average air temperature for January and February was over 6 °C higher than the 1981–2010 mean (Copernicus Climate Change Service, ECMWF). In this study we investigated how the exceptionally warm winter of 2019–2020 affected ENFs in Europe and whether increasing winter temperature increased or decreased the carbon uptake of the forest. Our objectives were to (1) evaluate the relative change in air and soil temperature and incoming radiation during the winter of 2019–2020, compared to a 6-year reference period of 2014–2019; (2) quantify the relative changes in the winter CO_2 fluxes across coniferous sites with available ecosystem-level CO_2 flux measurements; (3) tease apart the contribution of air temperature versus soil temperature versus solar radiation to changes in CO_2 fluxes during the warm winter; (4) test the sensitivity of CO_2 fluxes to each of the climatic drivers; and (5) test if the sensitivity of CO_2 fluxes to temperature changed during the warmer winter compared to previous years. Our hypothesis was that warming in winter will lead to a larger negative effect on net ecosystem productivity (i.e., higher CO_2 emissions) across colder forests due to increased ecosystem respiration. We addressed these objectives and tested our hypothesis by exploring ecosystem-level CO_2 fluxes measured with the eddy covariance method over 98 site years in 14 evergreen needleleaf forests distributed from the boreal to the Mediterranean regions of Europe.

2 Material and methods

2.1 Site description

We selected 14 evergreen needleleaf forests where continuous CO_2 fluxes and meteorological measurements were available for at least 6 years until the end of 2020. Selected sites were located from the northern to the southern edge of ENF forest distribution in Europe (Fig. 1). The most northern site studied is located in Sweden at 64.2° N (SE-Svb), and the most southern site is in Italy at 43.7° N (IT-SR2). Mean annual air temperature across the sites varies between 1.8 °C (at SE-Ros and SE-Svb) and 15.4 °C (at IT-SR2). Mean annual total precipitation varies from 527 mm (at SE-Nor) to 1316 mm (at CZ-BK1). Elevation ranges from 4 m a.s.l. (at IT-SR2) to 1730 m a.s.l. (at IT-Ren). CZ-BK1 has the largest leaf area index (LAI; 4.52 ± 0.09 SE), and SE-Ros has the smallest (2.59 ± 0.09). Table 1 summarizes the description of sites including their dominant canopy species.

2.2 Dataset

We used the eddy covariance dataset for the warm winter of 2020 processed with the FLUXNET pipeline (compatible with the FLUXNET2015 collection) in this study

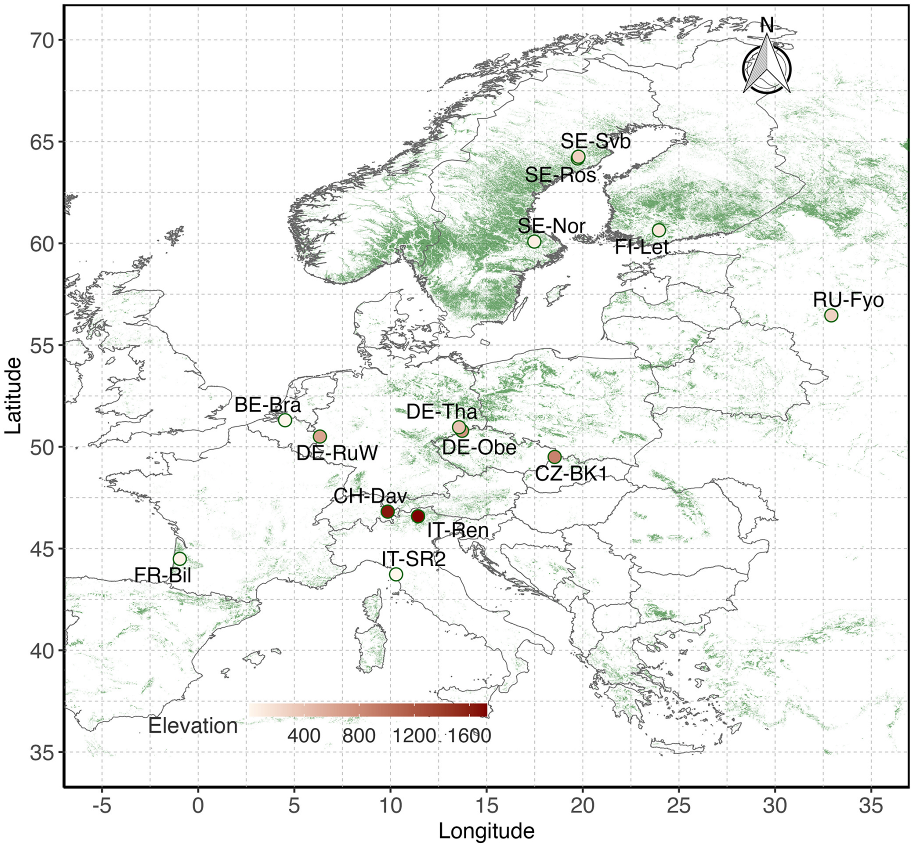

Figure 1. Location of the 14 evergreen needleleaf forest (ENF) sites included in this study. Basemap is the MODIS Land Cover product (MOD12Q1, 500 m spatial resolution) showing the distribution of ENFs in Europe in 2020. Elevation of the sites ranges from 4 m a.s.l. (IT-SR2) to 1735 m a.s.l. (IT-Ren).

(Warm Winter 2020 Team and ICOS Ecosystem Thematic Centre, 2022; https://www.icos-cp.eu/data-products/2G60-ZHAK, last access: 10 July 2024) (Pastorello et al., 2020). We included the analysis of soil and air temperature during the spring season at each site to check for any significant changes in the climate immediately after the winter season. Winter months included December, January, and February, and spring months included March, April, and May. The 6-year reference period was from 2014–2019. This period was selected to have sufficient temporal overlap between the sites. Net ecosystem exchange (NEE) quality-checked with a constant friction velocity (u^*) threshold was used for all sites (NEE_CUT_REF) (Shekhar et al., 2023). For an easier interpretation, we present net ecosystem exchange as net ecosystem productivity (NEP = −NEE), where a negative NEP indicates that the forest is a net source and positive NEP indicates that the forest is a net sink of CO_2 (Chapin et al., 2006).

In terms of climatic variables we selected those that overlapped in data availability across all sites during the study period. These included incoming shortwave radiation (R_g), air temperature (T_{air}), soil temperature at 5 cm (T_{soil}), and precipitation and topsoil water content. Given that continuous long-term snow depth measurements were not available at all sites, we used remotely sensed snow depth products to quantify mean snow depth and snow depth anomalies in winter 2020. The snow depth data were derived from the simulation of the Famine Early Warning System Network (FEWS NET) Land Data Assimilation System (FLDAS) (McNally et al., 2017). FLDAS data are produced from the Noah version 3.6.1 land surface model (LSM) at a monthly resolution with a global coverage at a spatial resolution of $0.1^\circ \times 0.1^\circ$ (approx. 10 km × 10 km) (Kumar et al., 2013) and have been used in the past to study global spatiotemporal patterns of snow depth and cover (Notarnicola, 2022). For snow cover we used the MODIS/Terra (MOD10A2) and MODIS/Aqua (MYD10A2) (Hall and Riggs, 2021) Snow Cover 8-Day L3 Global 500m SIN Grid, Version 6, dataset, which provides maximum snow cover extent at 8 d temporal resolution and 500 m spatial resolution. As a quality check, we compared the measured snow depth against the remotely sensed snow depth for one site (DE-Tha) for which measurements were available during the study period and found a reasonable agreement between the two datasets ($r = 0.86$, $p<0.001$). For each forest site, we derived the average (2014–2019) leaf area index (LAI) from the LAI Collection 300 m Version 1.1 product (LAI300) provided by the Copernicus Global Land

Table 1. Description of the 14 ENF study sites. Mean annual temperature and total precipitation refer to the 2014–2019 period. Mean number of days with snow cover for each site is based on the MODIS satellite observations. Sites are listed in decreasing order of mean annual temperature.

Site ID	Latitude (°)	Longitude (°)	Altitude (m a.s.l.)	Canopy species (dominant first)	Mean annual temperature (°C)	Mean annual precipitation (mm)	Number of days with snow cover
IT-SR2	43.7020	10.2909	4	*Pinus pinea*	15.7	950	0
FR-Bil	44.4936	−0.9560	39	*Pinus pinaster*	14.1	930	11
BE-Bra	51.3076	4.5198	16	*Pinus sylvestris*	11.5	750	20
DE-Tha	50.9625	13.5651	385	*Picea abies*	10.2	843	41
DE-RuW	50.5049	6.3310	610	*Picea abies*	8.7	1250	50
DE-Obe	50.7866	13.7212	734	*Picea abies*	7.4	996	90
SE-Nor	60.0864	17.4795	45	Mixed (*Pinus sylvestris*, *Picea abies*)	7.2	527	89
CZ-Bk1	49.5020	18.5368	875	*Picea abies*	7.1	1316	71
RU-Fyo	56.4615	32.9220	265	Mixed (*Picea abies, Betula pubescens*)	6.1	711	58
FI-Let	60.6418	23.9595	111	Mixed (*Pinus sylvestris*, *Picea abies*, *Betula pubescens*)	5.9	627	99
IT-Ren	46.5868	11.4336	1735	*Picea abies*	5.5	809	112
CH-Dav	46.8153	9.8559	1639	*Picea abies*	4.8	1062	139
SE-Ros	64.1725	19.738	160	*Pinus sylvestris*	4.0	614	102
SE-Svb	64.2561	19.774	267	Mixed (*Pinus sylvestris*, *Picea abies*, *Betula pubescens*)	3.2	614	106

Service (Fuster et al., 2020). The average LAI was estimated for each site during the mean net CO_2 uptake period. Following Shekhar et al. (2023), the start of the net carbon uptake period was defined as when daily NEP crosses from negative to positive and the end is the inverse.

2.3 Statistical analysis

We compared average daily and daytime (when $R_g > 10\,\mathrm{W\,m^{-2}}$ and 08:00–18:00 local time) means of each variable (v; climate drivers, CO_2 fluxes) during the winter and spring of 2020 to the mean from a 6-year reference period (2014–2019) using a t test ($p<0.05$). Daily means of each variable were calculated only using the measured and good-quality gap-filled half-hourly data (variable quality control = 0 or 1). To understand the major drivers of winter NEP, R_{eco}, and GPP for each forest site, we derived the conditional variable importance ($\mathrm{CVI_v}$) of each predictor variable (R_g, T_{air}, and T_{soil}) based on a random forest regression model built for the site (Breiman, 2001). For training the random forest model of R_{eco}, we additionally used GPP as an explanatory variable. In addition to the influence of abiotic drivers, the empirical relationship between photosynthesis (and thus GPP) and ecosystem respiration in forests has been established by a large body of research (Brüggemann et al., 2011; Koerner, 2013; Migliavacca et al., 2011; Shekhar et al., 2024). Soil water content (SWC) was removed from the drivers analysis (1) because of its negligible effect on the overall model (see details below), (2) since not all sites had complete measurements throughout the study period, (3) and because soil water content measurements at freezing soil temperature levels are not reliable and we observed that for several sites soil temperature in winter remained near or below 0 °C (Fig. S1). The effect of soil water content on the random forest (RF) model proved to be negligible after we compared the random forest results once with and once without SWC. The comparison revealed that the difference in the variance explained (R^2) was less than 3 %, indicating a negligible improvement in model performance based on the percentage of variance explained (see Fig. S2).

We tuned the random forest model by iterating the "n_{tree}" parameter (number of trees to grow) from 100 to 500 with steps of 50 and "m_{try}" parameter (number of variables to try at each split) from 1 to 3 with steps of 1 and chose the parameter ($n_{\mathrm{tree}} = 300$ and $m_{\mathrm{try}} = 2$) with the minimum mean square error. $\mathrm{CVI_v}$ accounts for the correlation between the predictor variables and was calculated using the `party` R package (Hothorn et al., 2006). Based on a 7 d moving window (centered on the central value of the window) we calculated the mean daily (and daytime) NEP, T_{air}, R_{g}, and T_{soil}. To compare the $\mathrm{CVI_v}$ across sites, for each site we calculated the relative CVI (RCVI) for each variable as per Eq. (1).

$$\mathrm{RCVI_v}\,(\%) = \frac{\mathrm{CVI_v}}{\sum \mathrm{CVI_v}} \times 100, \tag{1}$$

where $\sum \mathrm{CVI_v}$ is the sum of the $\mathrm{CVI_v}$ of all variables used in the model. We expressed changes in the variable during 2020 (v_{2020}) and the reference period ($v_{\mathrm{reference}}$) based on its relative anomaly (Δv_{r}) and absolute anomaly (Δv_{a}) as per Eqs. (2) and (3).

$$\Delta v_{\mathrm{r}}\,(\%) = \frac{v_{2020} - v_{\mathrm{reference}}}{|v_{\mathrm{reference}}|} \times 100 \tag{2}$$

$$\Delta v_a = v_{2020} - \underline{v}_{\mathrm{reference}} \tag{3}$$

To better understand how absolute anomalies in different variables (R_g, T_{air}, and T_{soil}) contributed to variations in ΔNEP, we applied the RCVI (as described in Eq. 2) derived from a random forest regression model. This model used ΔNEP as the response variable and R_g, T_{air}, and T_{soil} as predictors, with hyperparameters set to $n_{\mathrm{tree}} = 100$ and $m_{\mathrm{try}} = 3$ (optimized for the lowest mean squared error). The analysis was conducted at each site, with a minimum of 80 d of data points. The percent variance explained of the model (r^2) was based on the out-of-bag estimates. The sensitivity of NEP anomalies in winter (ΔNEP) to anomalies of climate drivers (R_g, T_{air}, and T_{soil}) was quantified as the slope of ΔR_g, ΔT_{air}, and ΔT_{soil} when regressed with ΔNEP using a multivariate linear regression ($\Delta\mathrm{NEP} \sim \Delta R_g + \Delta T_{\mathrm{air}} + \Delta T_{\mathrm{soil}}$).

3 Results

3.1 Conditions of the warm winter of 2019–2020 across different sites

According to the in situ data, compared to the reference period (2014–2019), winter 2020 was the warmest winter across 10 sites. At seven sites, the winter was also drier than normal (Fig. S3). Positive air temperature anomalies in winter 2020 were significantly larger at sites with a lower mean (2014–2019) air temperature ($p<0.05$, $r = -0.53$), with the largest significant anomaly of 4.79 °C at RU-Fyo and lowest significant positive anomaly of 0.87 °C observed at IT-SR2 (Fig. 2). Incoming shortwave radiation did not change significantly across any of the sites during the warm winter (data not shown here).

The average number of snow cover days per year was highly variable across the study sites (Table 1). The southernmost site studied here (IT-SR2) has no snow cover in winter, while the sub-Alpine forest in Switzerland (CH-Dav) has snow cover on 139 $\mathrm{d\,yr^{-1}}$ on average (Table 1). At those sites with consistent snow cover in winter (11 out of 14 sites), snow depth declined at 9 out of 11 sites during the warm winter of 2020, and this reduction was considerable at FI-Let, RU-Fyo, SE-Nor, DE-Obe, DE-RuW, and DE-Tha (Fig. 3). At SE-Svb, FI-Let, and DE-Obe soil temperature at 5 cm was continuously above the freezing level in winter 2020 (Fig. S1), unlike the mean conditions at the sites where soil temperature fluctuates around 0 °C in winter. Changes in air and soil temperature were more significant in winter than in spring (Fig. 2), which is the reason why we focus on the effect of winter warming on CO_2 fluxes.

3.2 Effect of climate drivers on winter CO_2 fluxes

The annual NEP of the ENFs varied from a maximum sink (± SD) of 797 (± 320) $\mathrm{g\,C\,m^{-2}\,yr^{-1}}$ (CZ-BK1) to a maximum source of −311 (± 93) $\mathrm{g\,C\,m^{-2}\,yr^{-1}}$ (SE-Nor) during the 6-year reference period (2014–2019) (Table 2). Interannual variation in NEP was largest at CZ-BK1 (320 $\mathrm{g\,C\,m^{-2}\,yr^{-1}}$) and lowest at SE-Svb (35 $\mathrm{g\,C\,m^{-2}\,yr^{-1}}$) (Table 2). The length of the net CO_2 uptake period was on average 178 d but varied between the sites from 105 d (at RU-Fyo) to 315 d (at DE-RuW) (Table 2). Except FR-Bil and DE-RuW, all sites were a CO_2 source in winter under reference conditions (Table S1).

During the warm winter of 2020, mean daily NEP (i.e., annual winter CO_2 sink or source strength) changed significantly ($p<0.05$) at 9 out of the 14 sites (BE-Bra, CZ-BK1, DE-Obe, FI-Let, IT-Ren, IT-SR2, SE-Svb, SE-Nor, and RU-Fyo, grouped together as the "affected" sites) compared to the 2014–2019 reference period, with changes in both positive and negative directions (Fig. 4). For example, at BE-Bra, DE-Obe, IT-Ren, SE-Svb, and FI-Let, the forest became a significantly larger source of CO_2 in winter 2020, while at SE-Nor, CZ-BK1, and RU-Fyo the forest shifted towards being a smaller source for CO_2 and at IT-SR2 it turned into a net sink in winter 2020 (Fig. 4, Table S1). IT-SR2 showed the largest increased daily NEP in winter (331 %), and BE-Bra showed the largest decline in daily NEP (−98 %) (Fig. 4). During the warm winter, ecosystem respiration (approximated by nighttime NEP) increased significantly across 10 out of the 14 sites, indicated by a negative anomaly in nighttime NEP (Fig. 4). Daytime NEP however (dominated by productivity) increased significantly with warming at only five sites (Fig. 4).

Figures 5–7 show the relationship between air temperature, soil temperature, and incoming shortwave radiation with NEP. Winter CO_2 fluxes in general (for the reference period of 2014–2019) showed a clear decline in NEP in response to an increase in soil temperature across several sites (SE-Svb, SE-Ros, FI-Let, SE-Nor, DE-Obe, BE-Bra, IT-SR2) (Fig. 7).

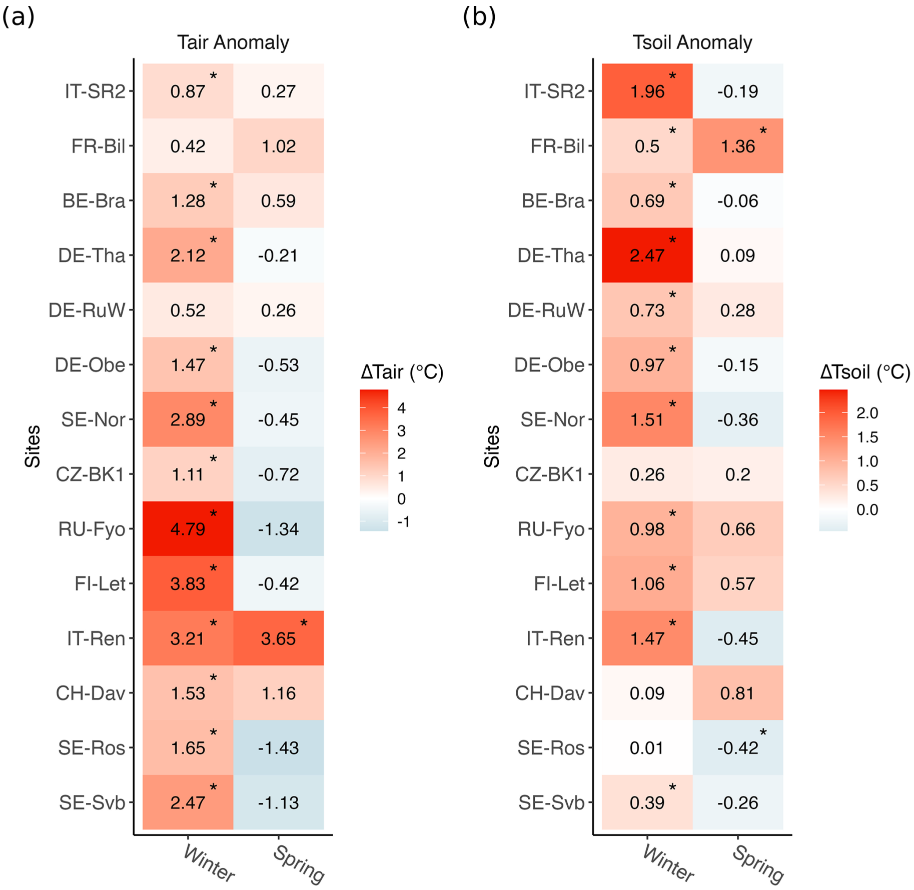

Figure 2. Seasonal changes in air temperature (T_{air}) and soil temperature (T_{soil}) in 2020 compared to the 6-year reference period (2014–2019). Asterisks mark where means in 2020 were significantly different from the reference period ($p<0.05$). Anomalies were calculated from daily values. Sites are listed from the top to the bottom in decreasing order of site mean annual air temperature.

Table 2. Mean total annual net ecosystem productivity (NEP) and the standard deviation (interannual variation) during the reference period (2014 and 2019). The start of the net carbon uptake period (start of season, SOS; day of year, DOY) is when daily NEP changes from negative to positive, and the end (end of season, EOS) is the inverse (following Shekhar et al., 2023). Sites are listed in decreasing order of mean annual air temperature.

Site ID	NEP (± SD) ($\mathrm{g\,C\,m^{-2}\,yr^{-1}}$)	SOS (DOY)	EOS (DOY)	Net carbon uptake period (d)
IT-SR2	197 (± 67)	35	200	165
FR-Bil	324 (± 103)	20	215	195
BE-Bra	279 (± 158)	95	270	175
DE-Tha	484 (± 88)	55	305	250
DE-RuW	597 (± 155)	1	315	315
DE-Obe	251 (± 147)	75	265	190
SE-Nor	-311 (± 93)	90	200	110
CZ-Bk1	797 (± 320)	70	310	240
RU-Fyo	25 (± 50)	95	200	105
FI-Let	-113 (± 123)	100	230	130
IT-Ren	675 (± 70)	75	305	230
CH-Dav	231 (± 139)	80	280	200
SE-Ros	320 (± 136)	95	255	160
SE-Svb	163 (± 35)	95	240	145

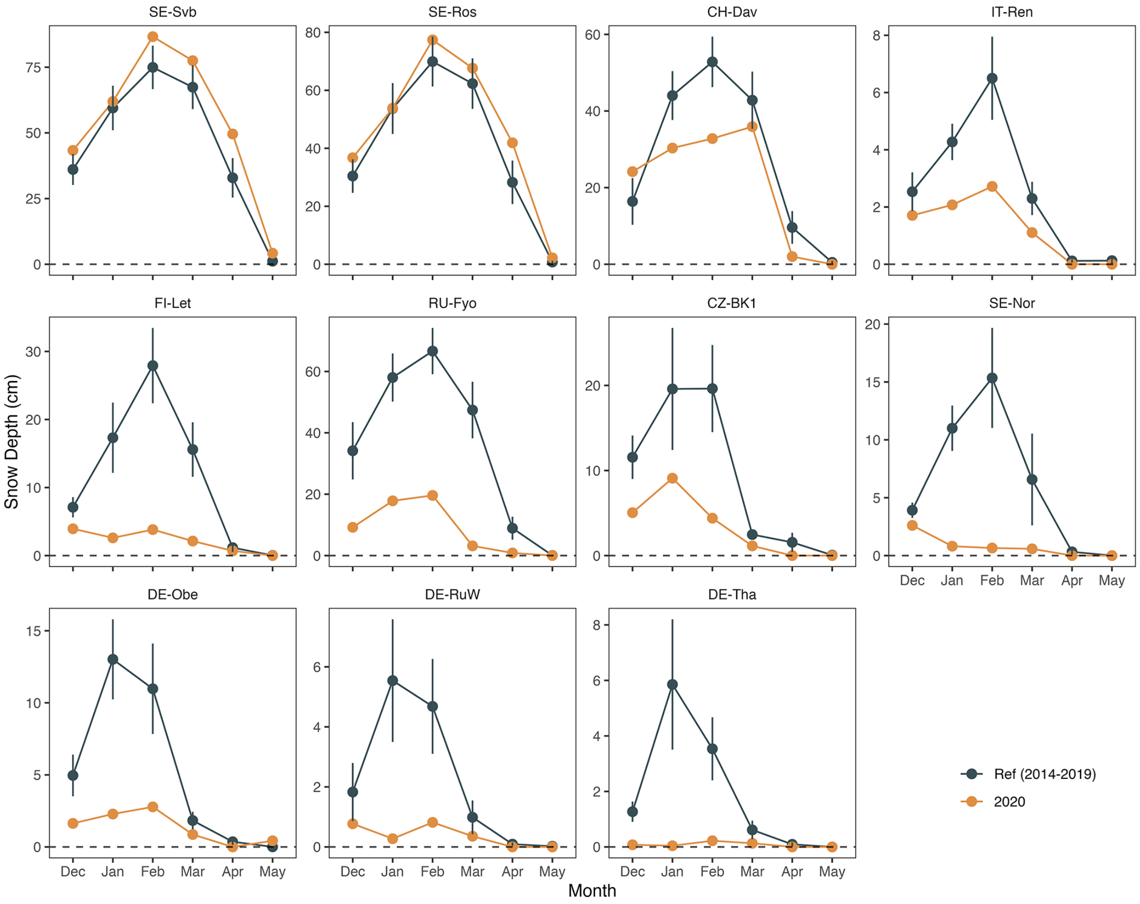

Figure 3. December–May snow depth changes in winter 2020 compared to the average winters during the reference period (2014–2019). Note that only 11 out of the 14 sites have persistent snow cover in winter. Sites are ordered from the top left to the right by increasing the site mean temperature (SE-Svb coldest and DE-Tha warmest).

While the response of NEP to R_g was more consistent across sites, the effect of soil and air temperature on NEP varied largely across sites. The average variation explained by the random forest regression for NEP in winter was 78 % (Fig. S4). The relative importance results of the random forest regression analysis showed that across tested variables, R_g generally had the largest effect on NEP. However, with a decrease in the site baseline (i.e., mean) temperature, the effect of R_g declined (Fig. 8). For example, at the three coldest sites (SE-Svb, CH-Dav, IT-Ren) R_g had a relative importance of 52 %, 23 %, and 41 % for the variations in NEP respectively, while at the three warmest sites (IT-SR2, FR-Bil, BE-Bra), R_g had a relative importance of 73 %, 81 %, and 58 % for NEP respectively (Fig. 8). When looking into partitioned fluxes, radiation dominated the effect on winter GPP and temperature dominated the effect on winter respiration fluxes (Fig. 8). Particularly at the colder sites was the effect of radiation the least important (Fig. 8).

3.3 Effect of warming on NEP anomalies

At warmer sites (low latitude or altitude < 1000 m a.s.l.) where NEP showed significant changes in winter 2020 (IT-SR2, BE-Bra, DE-Obe), the average NEP anomaly increased by 75 %. Conversely, at colder sites where NEP significantly changed in winter 2020 (SE-Nor, CZ-BK1, RU-Fyo, FI-Let, IT-Ren, SE-Svb), the average NEP anomaly decreased by 8.8 %, indicating reduced net carbon uptake (Fig. 4). Overall, at sites where daily NEP differed significantly during the warm winter, NEP increased at only three sites, while it declined significantly at the remaining six sites (Fig. 4). Changes in NEP are attributed only to changes in climatic factors because the forests did not undergo significant changes in the canopy density, except at FI-Let. While FI-Let was affected by a partial cut in 2016 (Korkiakoski et al., 2019, 2020), winter fluxes remained relatively stable in all pre- and post-harvest years as the partial cut affected mostly the summer fluxes (data not shown here).

Figure 9 shows the sensitivity of NEP anomalies to anomalies of air temperature, soil temperature, and radiation across

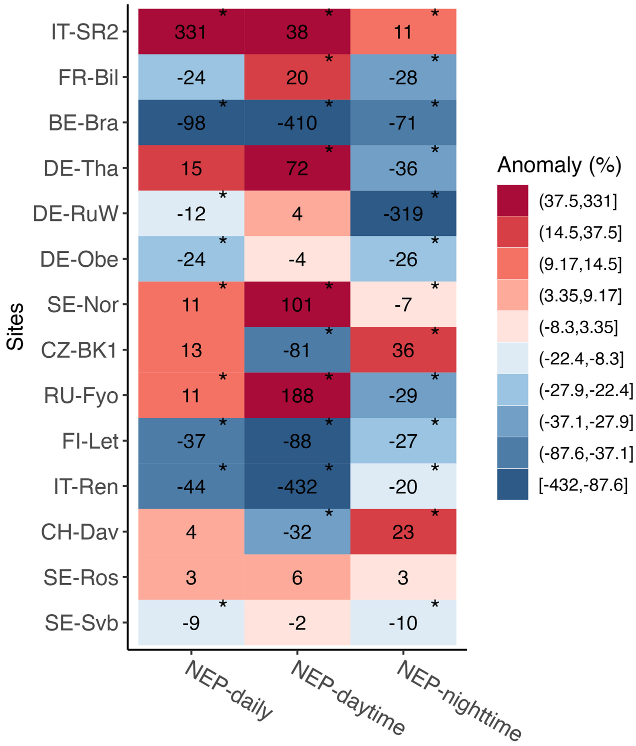

Figure 4. Relative change (anomaly, %) in mean daily, mean nighttime, and mean daytime NEP in winter 2020 compared to the 6-year reference winters (2014–2019). Asterisks mark where the mean in 2020 was significantly different from the reference period ($p<0.05$). Positive NEP change indicates increased net uptake (due to increased uptake or reduced emission), and negative change indicates decreased net uptake (due to reduced uptake or increased emission). Sites are listed from the top to the bottom in decreasing order of mean annual air temperature.

different sites. Overall, the sensitivity of NEP anomalies to soil temperature anomalies was larger than to anomalies of air temperature and radiation as shown by the test of the slope of change in NEP anomalies (Fig. 9).

While the relationship between air temperature and soil temperature was stronger than the relationship between radiation and air temperature during the winter, we observed large variability in the coupling between soil and air temperature across the sites, as is shown in Table 3.

4 Discussion

4.1 Warming of the air and the soil in winter

We tested how climate variables and CO_2 fluxes deviated from a reference period (2014–2019) during the warm winter of 2020 across 14 evergreen needleleaf forest sites distributed from the north to the south of Europe (from Sweden to Italy). The sites where winter 2020 was particularly warm and dry were not clustered in a certain climatic region; however we observed a consistent pattern that the warming of the air was more pronounced at the colder sites ($p<0.05$, $r=-0.53$, Figs. 2, S11).

Table 3. Pearson correlation coefficient between mean daily incoming shortwave radiation (R_g), air temperature (T_{air}), and soil temperature at 5 m (T_{soil}) at each site during the reference period (2014–2019). Sites are ordered by decreasing mean air temperature. Leaf area index (LAI) values are shown as mean across the study period ± standard error of the mean.

Site ID	$R_g - T_{air}$	$T_{air} - T_{soil}$	LAI ± SE
IT-SR2	0.69	0.97	3.12 (0.11)
FR-Bil	0.65	0.76	3.50 (0.08)
BE-Bra	0.67	0.92	4.42 (0.13)
DE-Tha	0.73	0.96	4.04 (0.19)
DE-RuW	0.59	0.83	2.99 (0.22)
DE-Obe	0.72	0.94	3.69 (0.21)
SE-Nor	0.71	0.90	3.08 (0.09)
CZ-Bk1	0.72	0.92	4.52 (0.09)
RU-Fyo	0.74	0.78	4.06 (0.14)
FI-Let	0.66	0.88	3.29 (0.27)
IT-Ren	0.64	0.84	3.54 (0.08)
CH-Dav	0.63	0.87	3.25 (0.12)
SE-Ros	0.69	0.77	2.59 (0.09)
SE-Svb	0.71	0.84	2.79 (0.12)

The strength of the coupling between the air and the soil temperature was not similar across all sites. In forests, topsoil temperature is directly affected by changes in air temperature; however, several underlying processes and properties modify the magnitude of decoupling between air and soil temperatures. This decoupling can reach up to 10 °C, depending on the season and the properties of the biome type (Lembrechts et al., 2022). These underlying factors and processes include for example (1) a vertically complex and horizontally continuous forest structure that leads to higher decoupling of the soil temperature from the air temperature; (2) soil moisture content as moisture increases the soil heat storage; (3) insulation by the litter or snow cover; (4) cloud cover, ground surface albedo, and the rate of evapotranspiration which collectively affect the radiation balance and energy exchange between the soil and the air; and (5) microtopography that affects the drainage of air (e.g., cool air drains in low-lying areas) (Guan et al., 2009; Lozano-Parra et al., 2018; De Frenne et al., 2021; Gril et al., 2023). Although the direct effect of canopy closure on snow distribution, accumulation, and melting in different periods was not tested here, it was evident that sites that had a larger LAI also showed a tighter coupling between air temperature and soil temperature ($p<0.05$, $r=0.69$, Table 3) as forest canopy structure influences the coupling of air and soil temperature in forest ecosystems, for example by shading the soil and reducing the snow depth beneath denser canopies (Woods et al., 2006; Gao et al., 2022). Snow cover plays a crucial role in regulat-

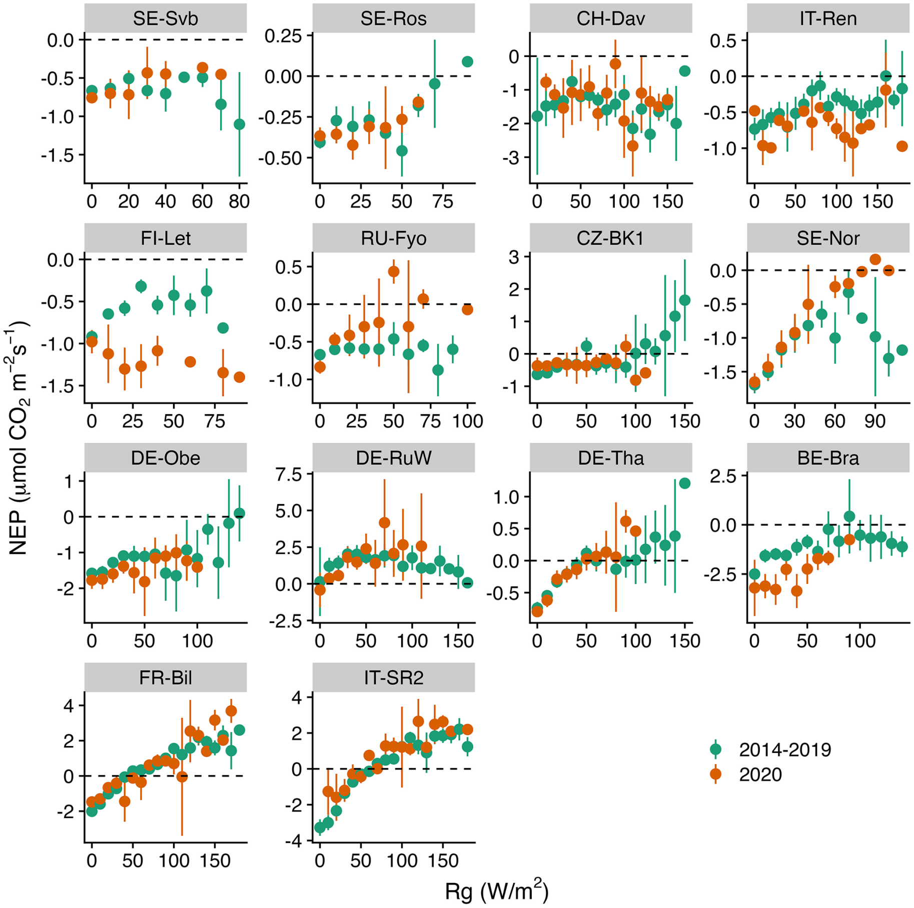

Figure 5. Comparison of the binned response of NEP versus R_g (incoming shortwave radiation) during the winters of the reference period (2014–2019) and winter 2020 across all sites (arranged from the top left to the bottom based on increasing mean air temperature). The daily mean NEP is aggregated (mean ± 95 % CI as error bars, confidence interval) at $10\,\mathrm{W\,m^{-2}}$ R_g bins.

ing the coupling between soil and air temperatures due to its insulating properties (Liu et al., 2023). At the sites selected for this study, the coupling between air and soil temperatures also tended to weaken as snow depth increased, though the relationship was not statistically significant ($r = 0.46$, $p>0.05$). A more detailed analysis across a larger number of sites is required to test if this may be due to uncertainties in remotely estimating snow depth beneath the forest canopy.

4.2 Winter warming effect on forest CO_2 fluxes

Winter warming had both positive and negative effects on the net ecosystem productivity (NEP) of coniferous forests. However, at most sites, NEP declined during the warm winter. This variation can largely be attributed to the differential effects of warming on soil versus air temperatures (Bond-Lamberty and Thomson, 2010), which influence both soil respiration and tree CO_2 uptake. When soil temperatures rise above freezing, root activity and respiration increase. Meanwhile, tree productivity may respond to higher air temperatures, potentially enhancing CO_2 uptake. However, air warming alone, without corresponding soil warming, might not disrupt dormancy (Bowling et al., 2024) if the soil within the rooting zone remains frozen. For instance, at IT-Ren, where daytime NEP significantly declined during the warm winter, air temperatures rose by over 3.5 °C above normal but soil temperatures stayed at freezing levels (Fig. S1).

Our hypothesis was that warming in winter will lead to a larger negative effect on net ecosystem productivity (i.e., higher CO_2 emissions) across colder forests. While we observed that (1) across most sites winter emissions increased during the warm winter and (2) generally emissions in winter increase in response to an increase in soil temperature (observed at seven sites, Fig. 7), we did not find a link between warming of the air and increased emissions that would confirm this general hypothesis.

CO_2 fluxes are influenced by both temperature and light (Figs. S5–S9). However, evidence suggests that the temperature response of biochemical processes is shaped more by the plant's growth temperature than by the immediate temperature (Fürstenau Togashi et al., 2018). Moreover, the net ecosystem productivity (NEP) response to similar tempera-

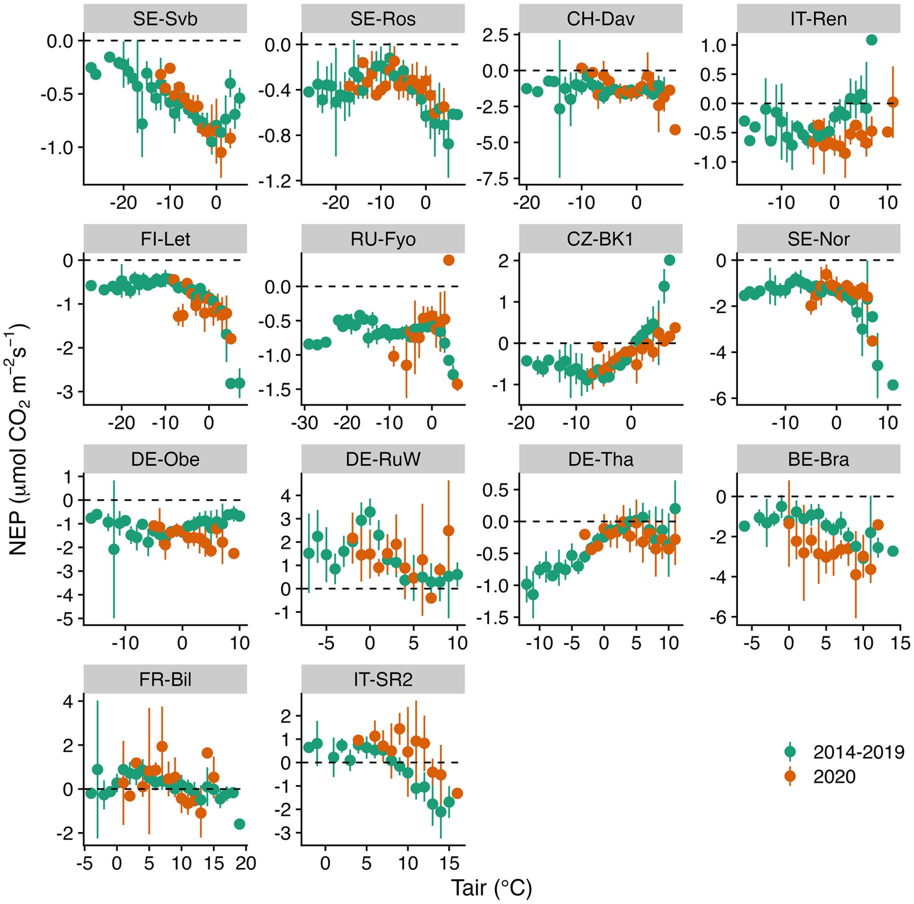

Figure 6. Comparison of the binned response of NEP versus T_{air} (air temperature) during the winters of the reference period (2014–2019) and winter 2020 across all sites (arranged from the top left to the bottom based on increasing mean air temperature). The daily mean NEP is aggregated (mean ± 95 % CI as error bars) at 1 °C T_{air} bins.

tures can vary seasonally, exhibiting a clear hysteresis effect, and is further influenced by environmental factors such as solar radiation and soil moisture (Niu et al., 2011). Across different sites, the sensitivity of NEP to temperature generally increases as site mean temperatures decrease. Once temperature is no longer a limiting factor at higher site mean temperatures, radiation becomes the dominant constraint on NEP (Running et al., 2004; Fig. 9).

Chamber-based observations from boreal forests indicate that snow depth and soil moisture significantly influence the temperature sensitivity of soil CO_2 fluxes, particularly due to the effects of freeze–thaw cycles on soil moisture content (Du et al., 2013). Warmer winters can lead to increased respiration rates and greater nutrient availability for trees, as thawed soils exhibit a higher Q_{10} than frozen soils, resulting in a more rapid increase in soil respiration in response to warming (Wang et al., 2014). However, this expected increase in respired CO_2 may be moderated by microbial carbon limitation, which can be alleviated through higher inputs of labile carbon from plant material and root exudates (Sullivan et al., 2020).

Furthermore, aboveground productivity tends to increase with rising temperatures (Figs. S6 and S7), contributing to enhanced autotrophic respiration. Warming during winter also affects the microbial communities responsible for decomposing labile and stable organic carbon in the soil, which can offset the respiration response to temperature and ultimately reduce overall soil respiration (Tian et al., 2021). The extent of belowground autotrophic respiration in response to warming, along with the supply of labile substrates through rhizodeposition and root exudates, plays a crucial role in determining net CO_2 fluxes under warming conditions (Nyberg et al., 2020). In our study, the sensitivity of ecosystem respiration (R_{eco}) to air temperature (Q_{10}) did not significantly change during the warm winter, remaining comparable to the Q_{10} observed during the reference period (Fig. S10).

A decrease in snowpack and increased soil freezing can have immediate short-term impacts on plant CO_2 uptake, but these changes may also lead to lasting negative effects on tree function (Repo et al., 2021). Particularly, sites with prolonged cold winter seasons could experience significant adverse effects from winter warming. Trees in northern lati-

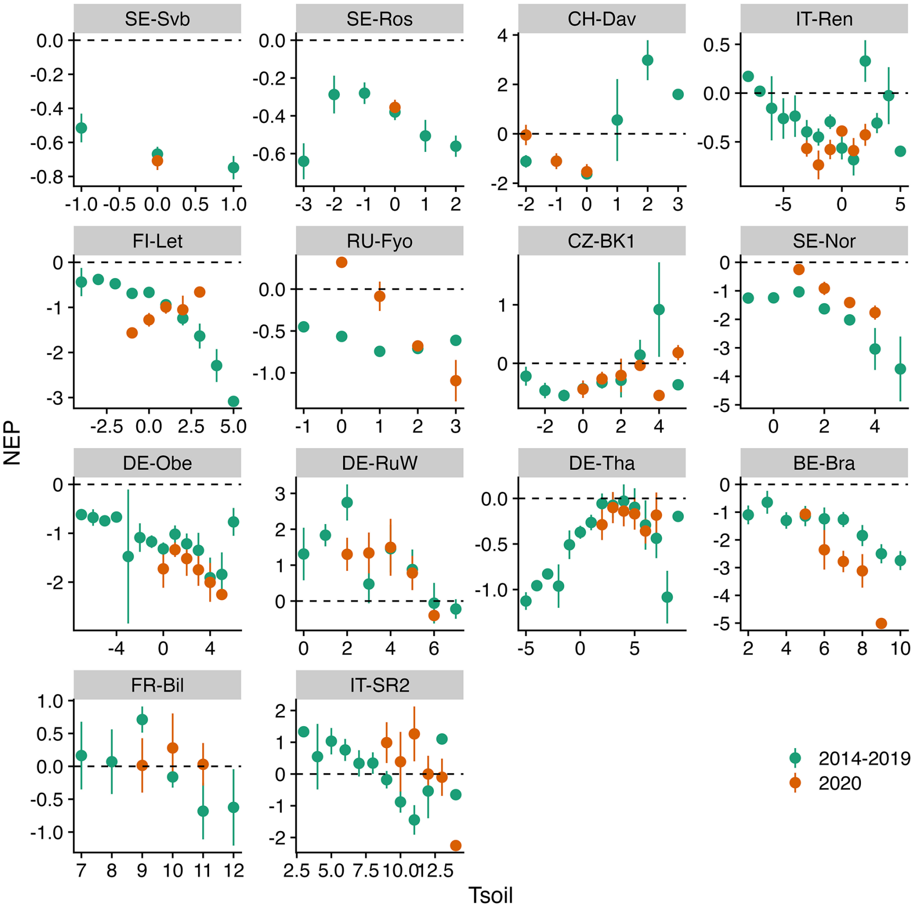

Figure 7. Comparison of the binned response of NEP versus T_{soil} (soil temperature) during the winters of the reference period (2014–2019) and winter 2020 across all sites (arranged from the top left to the bottom based on increasing mean air temperature). The daily mean NEP is aggregated (mean ± 95 % CI as error bars) at 1 °C T_{soil} bins.

tudes and at higher altitudes may be especially vulnerable to these changes, as their optimal growth temperatures are more sensitive to short-term temperature fluctuations. Conversely, in ecosystems with greater seasonal temperature variability, the optimal temperature range for growth is broader (Weng and Liao, 2010; Liu, 2020).

4.3 Winter tree physiology effect on CO$_2$ fluxes

Responses of coniferous species to soil warming can vary largely depending on the species' adaptive traits; the overall ecosystem context; and interactions with other environmental factors such as precipitation, temperature, and nutrient availability (Dawes et al., 2017; Oddi et al., 2022). The sites we studied here, although dominated by evergreen needleleaf species, consisted of different canopy species, and some sites were dominated by a mixture of species (Table 1). There can be significant differences in photosynthetic parameters across different species of evergreen conifers that would affect the tree and ecosystem response to warming (Fürstenau Togashi et al., 2018). The different responses of productivity to increased warming in ENFs can stem from differences in the quantity (and quality) of stored NSCs in the roots and the rate at which this C storage is mobilized within the tree during the warm winter (Bansal and Germino, 2009). Warmer temperatures and dry conditions in winter lead to stomatal closure and depletion of carbohydrate reserves for trees that are adapted to ample precipitation and conditions of low VPD (vapor pressure deficit) in winter, and this effect leads to reduced CO$_2$ uptake of trees during warmer winters (Earles et al., 2018).

Low temperatures are essential for signals that trigger the synthesis of soluble carbohydrates involved in osmotic and freezing protection against cold extremes (Chang et al., 2021) that otherwise impair the Calvin cycle by inhibiting the regeneration of ribulose bisphosphate (RuBP) and decrease the efficiency of ribulose-1,5-bisphosphate carboxylase/oxygenase (Rubisco) carboxylation (Ensminger et al., 2012; Crosatti et al., 2013). Non-structural carbohydrates (sugar and starch) that are accumulated during the growing season are utilized in winter to ensure the survival of trees (Zhu et al., 2012; Tixier et al., 2020), and failure to develop

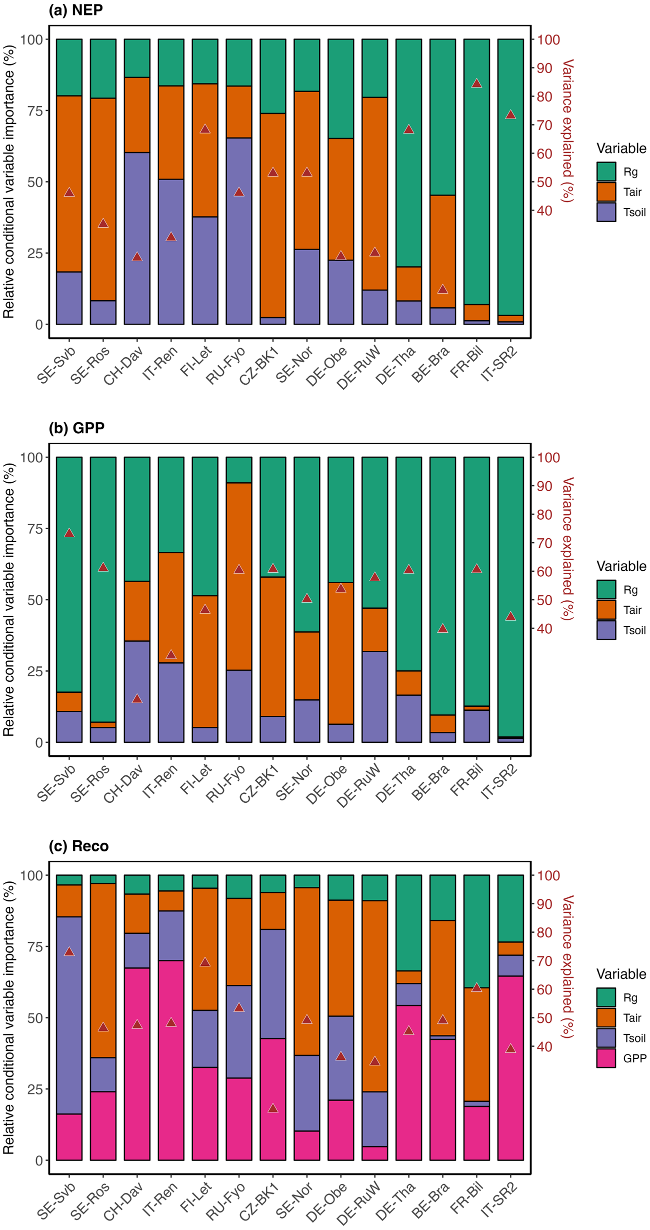

Figure 8. Relative conditional variable importance (RCVI, %) of three climatic variables for explaining the variance in daily winter NEP, GPP, and R_{eco} and the overall variability explained (r^2) (marked with red triangles) estimated from the random forest regression (RFR) analysis. The RFR model was trained on winter observations during the reference period (2014–2019). Sites are ordered by increasing site mean annual temperature (from left to right). For modeling R_{eco}, GPP was used as an additional predictor (see the methods section for more detail).

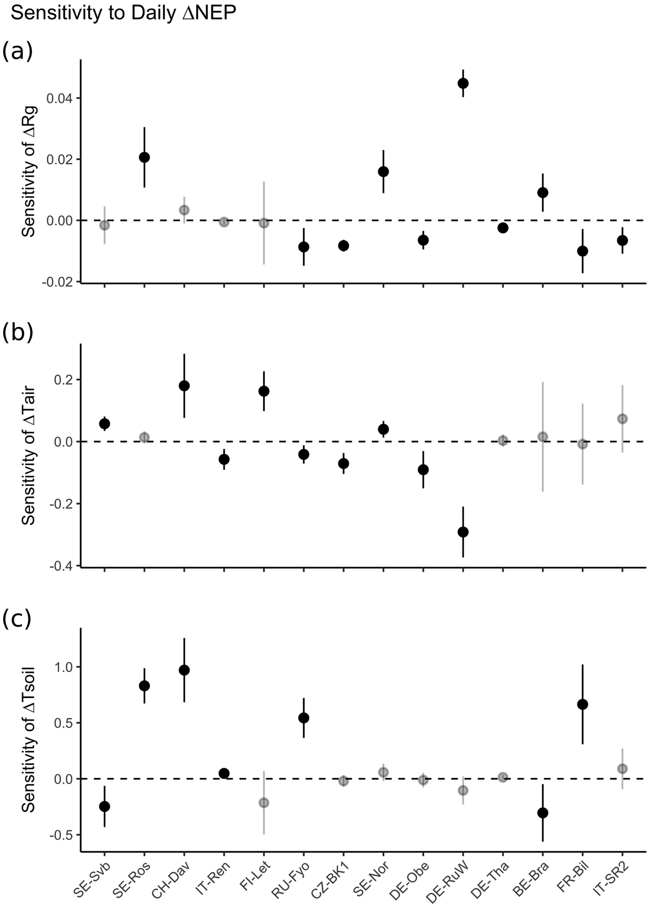

Figure 9. Sensitivity of NEP anomalies in winter (ΔNEP) to **(a)** anomalies of incoming solar radiation (ΔR_g), **(b)** anomalies of air temperature (ΔT_{air}), and **(c)** anomalies of soil temperature (ΔT_{soil}). The sensitivities represent the slope of ΔR_g, ΔT_{air}, and ΔT_{soil} when regressed with ΔNEP using a multivariate linear regression ($\Delta \mathrm{NEP} \sim \Delta R_g + \Delta T_{\mathrm{air}} + \Delta T_{\mathrm{soil}}$). The non-significant ($p<0.05$) sensitivity is shown as a transparent point. Error bar shows the 95 % CI of the slope obtained from the multivariate linear regression. Sites are ordered by increasing site mean air temperature (from left to right).

overwintering defenses can cause evergreen conifer needles to remain susceptible for example to photo-oxidative damage during frost events (Chang et al., 2016). Studies that combine ecosystem-scale flux measurements with tree-level observations have the potential to closely examine the adverse effects of winter warming on cold-adapted forests.

Our results represent the first analysis of the impact of winter warming on CO_2 fluxes in European evergreen needleleaf forests, highlighting the importance of understanding the various underlying mechanisms that influence forest CO_2 dynamics. Data on the responses of photosynthetic traits over ecologically relevant timescales (ranging from days to years) are limited. However, eddy covariance observations offer a valuable opportunity to construct long-term time series of canopy-level processes, enabling the investigation of the effects of extreme climatic conditions across all seasons. We also encourage further research that integrates long-term observations with plant-level experiments to explore how changes in winter functioning may influence trees' responses to early-season extremes, such as spring frost and drought, and to better understand the implications of these extremes for ecosystem carbon uptake.

5 Conclusions

Our study examined the effects of the warm winter of 2019–2020 on CO_2 fluxes in evergreen needleleaf forests across Europe. We showed that during wintertime net CO_2 emissions increased in response to warming across most sites. However, responses varied by location, with factors such as forest structure and local climatic conditions creating microclimates that either mitigated or intensified the impact of warming on CO_2 fluxes. By combining long-term eddy covariance data with plant-level experiments, we can gain valuable insights into how winter warming affects forest ecosystems. Future research should prioritize understanding the carryover effects of winter warming on tree responses to seasonal climatic extremes, as this knowledge is crucial for predicting how cold-adapted forests will respond to ongoing winter warming.

Data availability. The dataset used in this study is openly available from the ICOS Carbon Portal (https://doi.org/10.18160/2G60-ZHAK, Warm Winter 2020 Team and ICOS Ecosystem Thematic Centre, 2022).

Supplement. The supplement related to this article is available online at https://doi.org/10.5194/bg-22-1393-2025-supplement.

Author contributions. MG designed the study. MG and AS performed the data analysis. MG wrote the manuscript. All authors commented on the analysis and contributed substantially to the writing of the manuscript.

Competing interests. At least one of the (co-)authors is a member of the editorial board of *Biogeosciences*. The peer-review process was guided by an independent editor, and the authors also have no other competing interests to declare.

Acknowledgements. Mana Ghar acknowledges funding from the Swiss National Science Foundation project ICOS-CH Phase 3 (grant no. 20F120_198227). Thomas Grünwald acknowledges funding from the free state of Saxony (project Sicherstellung des Treibhausgasmonitorings an sächsischen ICOS-Standorten) and Bundesministerium für Bildung und Forschung (BMBF; project ICOS-D building phase). Bert Gielen and Marilyn Roland acknowledge the Research Foundation – Flanders (FWO) for the support of ICOS research infrastructure. Nina Buchmann acknowledges funding from the Schweizerischer Nationalfonds zur Förderung der Wissenschaftlichen Forschung (SNF) for ICOS-CH Phase 2 (grant no. 20FI20_173691) and EcoDrive (grant no. IZCOZ0_198094). Ladislav Šigut was supported by the Ministry of Education, Youth and Sports of the Czech Republic within the CzeCOS program (grant no. LM2023048). Ankit Shekhar acknowledges funding from SNF project EcoDrive (grant no. IZCOZ0_198094). We acknowledge the ICOS research infrastructure for data provision.

Financial support. This research has been supported by the Schweizerischer Nationalfonds zur Förderung der Wissenschaftlichen Forschung (grant no. 20F120_198227); the Freistaat Sachsen (Sicherstellung des Treibhausgasmonitorings an sächsischen ICOS-Standorten); the Bundesministerium für Bildung und Forschung (ICOS-D); the Schweizerischer Nationalfonds zur Förderung der Wissenschaftlichen Forschung (grant no. 20FI20_173691); the Schweizerischer Nationalfonds zur Förderung der Wissenschaftlichen Forschung (grant no. IZCOZ0_198094); and the Ministerstvo Školství, Mládeže a Tělovýchovy (grant no. LM2023048).

Review statement. This paper was edited by Andrew Feldman and reviewed by Jonas Lembrechts and one anonymous referee.

References

Bansal, S. and Germino, M. J.: Temporal variation of nonstructural carbohydrates in montane conifers: similarities and differences among developmental stages, species and environmental conditions, Tree Physiol., 9, 559–568, https://doi.org/10.1093/treephys/tpn045, 2009.

Beer, C., Reichstein, M., Tomelleri, E., Ciais, P., Jung, M., Carvalhais, N., Rödenbeck, C., Arain, M. A., Baldocchi, D., Bonan, G. B., Bondeau, A., Cescatti, A., Lasslop, G., Lindroth, A., Lomas, M., Luyssaert, S., Margolis, H., Oleson, K. W., Roupsard, O., Veenendaal, E., Viovy, N., Williams, C., Woodward, F. I., and Papale, D.: Terrestrial gross carbon dioxide uptake: global distribution and covariation with climate, Science, 329, 834–838, https://doi.org/10.1126/science.1184984, 2010.

Berry, J. and Björkman, O.: Photosynthetic response and adaptation to temperature in higher plants, Annu. Rev. Plant Physiol., 31, 491–543, 1980.

Bond-Lamberty, B. and Thomson, A.: Temperature-associated increases in the global soil respiration record, Nature, 464, 579–582, https://doi.org/10.1038/nature08930, 2010.

Bowling, D. R., Schädel, C., Smith, K. R., Richardson, A. D., Bahn, M., Arain, M. A., Varlagin, A., Ouimette, A. P., Frank, J. M., Barr, A. G., Mammarella, I., Šigut, L., Foord, V., Burns, S. P., Montagnani, L., Litvak, M. E., Munger, J. W., Ikawa, H., Hollinger, D. Y., Blanken, P. D., Ueyama, M., Matteucci, G., Bernhofer, C., Bohrer, G., Iwata, H., Ibrom, A., Pilegaard, K., Spittlehouse, D. L., Kobayashi, H., Desai, A. R., Staebler, R. M., and Black, T. A.: Phenology of photosynthesis in winter-dormant temperate and boreal forests: Long-term observations from flux towers and quantitative evaluation of phenology models, J. Geophys. Res.-Biogeo., 129, e2023JG007839, https://doi.org/10.1029/2023JG007839, 2024.

Breiman, L.: Random forests, Mach. Learn., 45, 5–32, https://doi.org/10.1023/A:1010933404324, 2001.

Brüggemann, N., Gessler, A., Kayler, Z., Keel, S. G., Badeck, F., Barthel, M., Boeckx, P., Buchmann, N., Brugnoli, E., Esperschütz, J., Gavrichkova, O., Ghashghaie, J., Gomez-Casanovas, N., Keitel, C., Knohl, A., Kuptz, D., Palacio, S., Salmon, Y., Uchida, Y., and Bahn, M.: Carbon allocation and carbon isotope fluxes in the plant soil-atmosphere continuum: a review, Biogeosciences, 8, 3457–3489, https://doi.org/10.5194/bg-8-3457-2011, 2011.

Chamberlain, C. J., Cook, B. I., García de Cortázar-Atauri, I., and Wolkovich, E. M.: Rethinking false spring risk, Glob. Change Biol., 25, 2209–2220, https://doi.org/10.1111/gcb.14642, 2019.

Chang, C. Y., Unda, F., Zubilewich, A., Mansfield, S. D., and Ensminger, I.: Sensitivity of cold acclimation to elevated autumn temperature in field-grown Pinus strobus seedlings, Front. Plant Sci., 6, 165, https://doi.org/10.3389/fpls.2015.00165, 2015.

Chang, C. Y., Fréchette, E., Unda, F., Mansfield, S. D., and Ensminger, I.: Elevated temperature and CO_2 stimulate late-season photosynthesis but impair cold hardening in pine, Plant Physiol., 172, 802–818, https://doi.org/10.1104/pp.16.00753, 2016.

Chang, C. Y.-Y., Bräutigam, K., Hüner, N. P. A., and Ensminger, I.: Champions of winter survival: cold acclimation and molecular regulation of cold hardiness in evergreen conifers, New Phytol., 229, 675–691, https://doi.org/10.1111/nph.16904, 2021.

Chapin III, F. S., Woodwell, G. M., Randerson, J. T., Rastetter, E. B., Lovett, G. M., Baldocchi, D. D., Clark, D. A., Harmon, M. E., Schimel, D. S., Valentini, R., Wirth, C., Aber, J. D., Cole, J. J., Goulden, M. L., Harden, J. W., Heimann, M., Howarth, R. W., Matson, P. A., McGuire, A. D., Melillo, J. M., Mooney, H. A., Neff, J. C., Houghton, R. A., Pace, M. L., Ryan, M. G., Running, S. W., Sala, O. E., Schlesinger, W. H., and Schulze, E.-D.: Reconciling carbon-cycle concepts, terminology, and methods, Ecosystems, 9, 1041–1050, https://doi.org/10.1007/s10021-005-0105-7, 2006.

Chen, S., Wang, J., Zhang, T., and Hu, Z.: Climatic, soil, and vegetation controls of the temperature sensitivity (Q_{10}) of soil respiration across terrestrial biomes, Global Ecol. Conserv., 22, e00955, https://doi.org/10.1016/j.gecco.2020.e00955, 2020.

Collalti, A., Tjoelker, M. G., Hoch, G., Mäkelä, A., Guidolotti, G., Heskel, M., Petit, G., Ryan, M. G., Battipaglia, G., Matteucci, G., and Prentice, I. C.: Plant respiration: controlled by photosynthesis or biomass?, Glob. Change Biol., 26, 1739–1753, https://doi.org/10.1111/gcb.14857, 2020.

Copernicus Climate Change Service (C3S): European State of the Climate 2020 – Warm Winter, https://climate.copernicus.eu/esotc/2020/warm-winter (last access: 17 February 2025), 2020.

Crosatti, C., Rizza, F., Badeck, F.-W., Mazzucotelli, E., and Cattivelli, L.: Harden the chloroplast to protect the plant, Physiol. Plant., 147, 55–63, https://doi.org/10.1111/ppl.12007, 2013.

Dawes, M. A., Schleppi, P., Hättenschwiler, S., Rixen, C., and Hagedorn, F.: Soil warming opens the nitrogen cycle at the alpine treeline, Glob. Change Biol., 23, 421–434, https://doi.org/10.1111/gcb.13365, 2017.

De Frenne, P., Lenoir, J., Luoto, M., Scheffers, B. R., Zellweger, F., Aalto, J., Ashcroft, M. B., Christiansen, D. M., Decocq, G., De Pauw, K., Govaert, S., Greiser, C., Gril, E., Hampe, A., Jucker, T., Klinges, D. H., Koelemeijer, I. A., Lembrechts, J. J., Marrec, R., Meeussen, C., Ogée, J., Tyystjärvi, V., Vangansbeke, P., and Hylander, K.: Forest microclimates and climate change: importance, drivers and future research agenda, Glob. Change Biol., 27, 2279–2297, https://doi.org/10.1111/gcb.15569, 2021.

Desai, A., Wohlfahrt, G., Zeeman, M. J., Katata, G., Eugster, W., Montagnani, L., Gianelle, D., Mauder, M., and Schmid, H. P.: Montane ecosystem productivity responds more to global circulation patterns than climatic trends, Environ. Res. Lett., 11, 024013, https://doi.org/10.1088/1748-9326/11/2/024013, 2016.

Du, E., Zhou, Z., Li, P., Jiang, L., Hu, X., and Fang, J.: Winter soil respiration during soil-freezing process in a boreal forest in Northeast China, J. Plant Ecol., 6, 349–357, https://doi.org/10.1093/jpe/rtt012, 2013.

Earles, J. M., Stevens, J. T., Sperling, O., Orozco, J., North, M. P., and Zwieniecki, M. A.: Extreme mid-winter drought weakens tree hydraulic–carbohydrate systems and slows growth, New Phytol., 219, 89–97, https://doi.org/10.1111/nph.15136, 2018.

Ensminger, I., Busch, F., and Huner, N. P. A.: Photostasis and cold acclimation: sensing low temperature through photosynthesis, Physiol. Plant., 126, 28–44, https://doi.org/10.1111/j.1399-3054.2006.00627.x, 2006.

Ensminger, I., Berninger, F., and Streb, P.: Response of photosynthesis to low temperature, in: Terrestrial Photosynthesis in a Changing Environment: A Molecular, Physiological, and Ecological Approach, edited by: Flexas, J., Loreto, F., and Medrano, H., Cambridge University Press, Cambridge, UK, 276–293, ISBN: 978-0-521-89941-3, 2012.

Fierer, N., Craine, J. M., McLauchlan, K., and Schimel, J. P.: Litter quality and the temperature sensitivity of decomposition, Ecology, 86, 320–326, 2005.

Friedlingstein, P., O'Sullivan, M., Jones, M. W., Andrew, R. M., Bakker, D. C. E., Hauck, J., Landschützer, P., Le Quéré, C., Luijkx, I. T., Peters, G. P., Peters, W., Pongratz, J., Schwingshackl, C., Sitch, S., Canadell, J. G., Ciais, P., Jackson, R. B., Alin, S. R., Anthoni, P., Barbero, L., Bates, N. R., Becker, M., Bellouin, N., Decharme, B., Bopp, L., Brasika, I. B. M., Cadule, P., Chamberlain, M. A., Chandra, N., Chau, T.-T.-T., Chevallier, F., Chini, L. P., Cronin, M., Dou, X., Enyo, K., Evans, W., Falk, S., Feely, R. A., Feng, L., Ford, D. J., Gasser, T., Ghattas, J., Gkritzalis, T., Grassi, G., Gregor, L., Gruber, N., Gürses, Ö., Harris, I., Hefner, M., Heinke, J., Houghton, R. A., Hurtt, G. C., Iida, Y., Ilyina, T., Jacobson, A. R., Jain, A., Jarníková, T., Jersild, A., Jiang, F., Jin, Z., Joos, F., Kato, E., Keeling, R. F., Kennedy, D., Klein Goldewijk, K., Knauer, J., Korsbakken, J. I., Körtzinger, A., Lan, X., Lefèvre, N., Li, H., Liu, J., Liu, Z., Ma, L., Marland, G., Mayot, N., McGuire, P. C., McKinley, G. A., Meyer, G., Morgan, E. J., Munro, D. R., Nakaoka, S.-I., Niwa, Y., O'Brien, K. M., Olsen, A., Omar, A. M., Ono, T., Paulsen, M., Pierrot, D., Pocock, K., Poulter, B., Powis, C. M., Rehder, G., Resplandy, L., Robertson, E., Rödenbeck, C., Rosan, T. M., Schwinger, J., Séférian, R., Smallman, T. L., Smith, S. M., Sospedra-Alfonso, R., Sun, Q., Sutton, A. J., Sweeney, C., Takao, S., Tans, P. P., Tian, H., Tilbrook, B., Tsujino, H., Tubiello, F., van der Werf, G. R., van Ooijen, E., Wanninkhof, R., Watanabe, M., Wimart-Rousseau, C., Yang, D., Yang, X., Yuan, W., Yue, X., Zaehle, S., Zeng, J., and Zheng, B.: Global Carbon Budget 2023, Earth Syst. Sci. Data, 15, 5301–5369, https://doi.org/10.5194/essd-15-5301-2023, 2023.

Forkel, M., Carvalhais, N., Rödenbeck, C., Keeling, R., Heimann, M., Thonicke, K., Zaehle, S., and Reichstein, M.: Enhanced seasonal CO_2 exchange caused by amplified plant productivity in northern ecosystems, Science, 351, 696–699, https://doi.org/10.1126/science.aac4971, 2016.

Fürstenau Togashi, H., Prentice, I. C., Atkin, O. K., Macfarlane, C., Prober, S. M., Bloomfield, K. J., and Evans, B. J.: Thermal acclimation of leaf photosynthetic traits in an evergreen woodland, consistent with the coordination hypothesis, Biogeosciences, 15, 3461–3474, https://doi.org/10.5194/bg-15-3461-2018, 2018.

Fuster, B., Sánchez-Zapero, J., Camacho, F., García-Santos, V., Verger, A., Lacaze, R., Weiss, M., Baret, F., and Smets, B.: Quality assessment of PROBA-V LAI, fAPAR and fCOVER collection 300 m products of Copernicus global land service, Remote Sens., 12, 1017, https://doi.org/10.3390/rs12061017, 2020.

Gao, Y., Shen, L., Cai, R., Wang, A., Yuan, F., Wu, J., Guan, D., and Yao, H.: Impact of forest canopy closure on snow processes in the Changbai Mountains, Northeast China, Front. Environ. Sci., 10, 929309, https://doi.org/10.3389/fenvs.2022.929309, 2022.

Gharun, M., Hörtnagl, L., Paul-Limoges, E., Ghiasi, S., Feigenwinter, I., Burri, S., Marquardt, K., Etzold, S., Zweifel, R., Eugster, W., and Buchmann, N.: Physiological response of Swiss ecosystems to 2018 drought across plant types and elevation, Philos. T. R. Soc. B, 375, 20190521, https://doi.org/10.1098/rstb.2019.0521, 2020.

Gharun, M., Shekhar, A., Xiao, J., Li, X., and Buchmann, N.: Effect of the 2022 summer drought across forest types in Europe, Biogeosciences, 21, 5481–5494, https://doi.org/10.5194/bg-21-5481-2024, 2024.

Gril, E., Spicher, F., Greiser, C., Ashcroft, M. B., Pincebourde, S., Durrieu, S., Nicolas, M., Richard, B., Decocq, G., Marrec, R., and Lenoir, J.: Slope and equilibrium: A parsimonious and flexible approach to model microclimate, Methods Ecol. Evol., 14, 885–897, https://doi.org/10.1111/2041-210X.14048, 2023.

Gu, L., Hanson, P. J., MacPost, A., and Olson, R. J.: The 2007 eastern US spring freeze: Increased cold damage in a warming world?, BioScience, 58, 253–262, https://doi.org/10.1641/B580311, 2008.

Guan, X., Huang, J., Guo, N., Bi, J., Wang, G., and Shi, H.: Variability of soil moisture and its relationship with surface albedo and soil thermal parameters over the Loess Plateau, Adv. Atmos. Sci., 26, 692–700, https://doi.org/10.1007/s00376-009-8198-0, 2009.

Haesen, S., Lembrechts, J. J., De Frenne, P., Lenoir, J., Aalto, J., Ashcroft, M. B., Kopecký, M., Luoto, M., Maclean, I., Nijs, I., Niittynen, P., van den Hoogen, J., Arriga, N., Brůna, J., Buchmann, N., Čiliak, M., Collalti, A., De Lombaerde, E., Descombes, P., and Van Meerbeek, K.: ForestTemp – Sub-canopy microclimate temperatures of European forests, Glob. Change Biol., 27, 6307–6319, https://doi.org/10.1111/gcb.15892, 2021.

Hall, D. K. and Riggs, G. A.: MODIS/Terra Snow Cover 8-Day L3 Global 500 m SIN Grid, Version 6, NASA National Snow and Ice Data Center Distributed Active Archive Center, https://doi.org/10.5067/MODIS/MOD10A2.006, 2021.

Hothorn, T., Hornik, K., and Zeileis, A.: Unbiased Recursive Partitioning: A Conditional Inference Framework, J. Comput. Graph. Stat., 15, 651–674, https://doi.org/10.1198/106186006X133933, 2006.

Hui, D., Luo, Y., and Katul, G.: Partitioning interannual variability in net ecosystem exchange between climatic variability and functional change, Tree Physiol., 23, 433–442, https://doi.org/10.1093/treephys/23.7.433, 2003.

IPCC: Climate Change 2014: Synthesis Report, Contribution of Working Groups I, II and III to the Fifth Assessment Report of the Intergovernmental Panel on Climate Change, edited by: Core Writing Team, Pachauri, R. K., and Meyer, L. A., IPCC, Geneva, Switzerland, 151 pp., 2014.

Karhu, K., Auffret, M. D., Dungait, J. A. J., Hopkins, D. W., Prosser, J. I., Singh, B. K., Subke, J.-A., Wookey, P. A., Ågren, G. I., Sebastià, M.-T., Gouriveau, F., Bergkvist, G., Meir, P., Nottingham, A. T., Salinas, N., and Hartley, I. P.: Temperature sensitivity of soil respiration rates enhanced by microbial community response, Nature, 513, 81–84, https://doi.org/10.1038/nature13604, 2014.

Korkiakoski, M., Tuovinen, J. P., Penttilä, T., Sarkkola, S., Ojanen, P., Minkkinen, K., Rainne, J., Laurila, T., and Lohila, A.: Greenhouse gas and energy fluxes in a boreal peatland forest after clear-cutting, Biogeosciences, 16, 3703–3723, https://doi.org/10.5194/bg-16-3703-2019, 2019.

Korkiakoski, M., Ojanen, P., Penttilä, I., Minkkinen, K., Sarkkola, S., Rainne, J., Laurila, T., and Lohila, A.: Impact of partial harvest on CH_4 and N_2O balances of a drained boreal peatland forest, Agr. Forest Meteorol., 295, 108168, https://doi.org/10.1016/j.agrformet.2020.108168, 2020.

Koerner, C.: Plant–environment interactions, in: Strasburger's Plant Sciences: Including Prokaryotes and Fungi, edited by: Bresinsky, A., Koerner, C., Kadereit, J. W., Neuhaus, G., and Sonnewald, U., Springer, Berlin, Heidelberg, 1065–1166, https://doi.org/10.1007/978-3-642-15518-5_12, 2013.

Kreyling, J., Grant, K., Hammerl, V., Arfin-Khan, M. A. S., Malyshev, A. V., Peñuelas, J., Pritsch, K., Sardans, J., Schloter, M., Schuerings, J., Jentsch, A., and Beierkuhnlein, C.: Winter warming is ecologically more relevant than summer warming in a cool-temperate grassland, Sci. Rep., 9, 14632, https://doi.org/10.1038/s41598-019-51221-w, 2019.

Kumar, S. V., Peters-Lidard, C. D., Mocko, D., and Tian, Y.: Multiscale evaluation of the improvements in surface snow simulation through terrain adjustments to radiation, J. Hydrometeorol., 14, 220–232, https://doi.org/10.1175/JHM-D-12-046.1, 2013.

Law, B. E., Baldocchi, D. D., and Anthoni, P. M.: Below-canopy and soil CO_2 fluxes in a ponderosa pine forest, Agr. Forest Meteorol., 94, 171–188, 1999.

Lembrechts, J. J., van den Hoogen, J., Aalto, J., Ashcroft, M. B., De Frenne, P., Kemppinen, J., Kopecký, M., Luoto, M., Maclean, I. M. D., Crowther, T. W., Bailey, J. J., Haesen, S., Klinges, D. H., Niittynen, P., Scheffers, B. R., Van Meerbeek, K., Aartsma, P., Abdalaze, O., Abedi, M., Aerts, R., Ahmadian, N., Ahrends, A., Alatalo, J. M., Alexander, J. M., Allonsius, C. N., Altman, J., Ammann, C., Andres, C., Andrews, C., Ardö, J., Arriga, N., Arzac, A., Aschero, V., Assis, R. L., Assmann, J. J., Bader, M. Y., Bahalkeh, K., Barančok, P., Barrio, I. C., Barros, A., Barthel, M., Basham, E. W., Bauters, M., Bazzichetto, M., Belelli Marchesini, L., Bell, M. C., Benavides, J. C., Benito Alonso, J. L., Berauer, B. J., Bjerke, J. W., Björk, R. G., Björkman, M. P., Björnsdóttir, K., Blonder, B., Boeckx, P., Boike, J., Bokhorst, S., Brum, B. N. S., Brůna, J., Buchmann, N., Buysse, P., Camargo, J. L., Campoe, O. C., Candan, O., Canessa, R., Cannone, N., Carbognani, M., Carnicer, J., Casanova-Katny, A., Cesarz, S., Chojnicki, B., Choler, P., Chown, S. L., Cifuentes, E. F., Čiliak, M., Contador, T., Convey, P., Cooper, E. J., Cremonese, E., Curasi, S. R., Curtis, R., Cutini, M., Dahlberg, C. J., Daskalova, G. N., de Pablo, M. A., Della Chiesa, S., Dengler, J., Deronde, B., Descombes, P., Di Cecco, V., Di Musciano, M., Dick, J., Dimarco, R. D., Dolezal, J., Dorrepaal, E., Dušek, J., Eisenhauer, N., Eklundh, L., Erickson, T. E., Erschbamer, B., Eugster, W., Ewers, R. M., Exton, D. A., Fanin, N., Fazlioglu, F., Feigenwinter, I., Fenu, G., Ferlian, O., Fernández Calzado, M. R., Fernández-Pascual, E., Finckh, M., Finger Higgens, R., Forte, T. G. W., Freeman, E. C., Frei, E. R., Fuentes-Lillo, E., García, R. A., García, M. B., Géron, C., Gharun, M., Ghosn, D., Gigauri, K., Gobin, A., Goded, I., Goeckede, M., Gottschall, F., Goulding, K., Govaert, S., Graae, B. J., Greenwood, S., Greiser, C., Grelle, A., Guénard, B., Guglielmin, M., Guillemot, J., Haase, P., Haider, S., Halbritter, A. H., Hamid, M., Hammerle, A., Hampe, A., Haugum, S. V., Hederová, L., Heinesch, B., Helfter, C., Hepenstrick, D., Herberich, M., Herbst, M., Hermanutz, L., Hik, D. S., Hoffrén, R., Homeier, J., Hörtnagl, L., Høye, T. T., Hrbacek, F., Hylander, K., Iwata, H., Jackowicz-Korczynski, M. A., Jactel, H., Järveoja, J., Jastrzębowski, S., Jentsch, A., Jiménez, J. J., Jónsdóttir, I. S., Jucker, T., Jump, A. S., Juszczak, R., Kanka, R., Kašpar, V., Kazakis, G., Kelly, J., Khuroo, A. A., Klemedtsson, L., Klisz, M., Kljun, N., Knohl, A., Kobler, J., Kollár, J., Kotowska, M. M., Kovács, B., Kreyling, J., Lamprecht, A., Lang, S. I., Larson, C., Larson, K., Laska, K., le Maire, G., Leihy, R. I., Lens, L., Liljebladh, B., Lohila, A., Lorite, J., Loubet, B., Lynn, J., Macek, M., Mackenzie, R., Magliulo, E., Maier, R., Malfasi, F., Máliš, F., Man, M., Manca, G., Manco, A., Manise, T., Manolaki, P., Marciniak, F., Matula, R., Mazzolari, A. C., Medinets, S., Medinets, V., Meeussen, C., Merinero, S., Mesquita, R. d. C. G., Meusburger, K., Meysman, F. J. R., Michaletz, S. T., Milbau, A., Moiseev, D., Moiseev, P., Mondoni, A., Monfries, R., Montagnani, L., Moriana-Armendariz, M., Morra di Cella, U., Mörsdorf, M., Mosedale, J. R., Muffler, L., Muñoz-Rojas, M., Myers, J. A., Myers-Smith, I. H., Nagy, L., Nardino, M., Naujokaitis-Lewis, I., Newling, E., Nicklas, L., Niedrist, G., Niessner, A., Nilsson, M. B., Normand, S., Nosetto, M. D., Nouvellon, Y., Nuñez, M. A., Ogaya, R., Ogée, J., Okello, J., Olejnik, J., Olesen, J. E., Opedal, Ø. H., Orsenigo, S., Palaj, A., Pampuch, T., Panov, A. V., Pärtel, M., Pastor, A., Pauchard, A., Pauli, H., Pavelka, M., Pearse, W. D., Peichl, M., Pellissier, L., Penczykowski, R. M., Penuelas, J., Petit Bon, M., Petraglia, A., Phartyal, S. S., Phoenix, G. K., Pio, C., Pitacco, A., Pitteloud, C., Plichta, R., Porro, F., Portillo-Estrada, M., Poulenard, J., Poyatos, R., Prokushkin, A. S., Puchalka, R., Pu?ca?, M., Radujković, D., Randall, K., Ratier Backes, A., Remmele, S., Remmers, W., Renault, D., Risch, A. C., Rixen, C., Robinson, S. A., Robroek, B. J. M., Rocha, A. V., Rossi, C., Rossi, G., Roupsard, O., Rubtsov, A. V., Saccone, P., Sagot, C., Sallo Bravo, J., Santos, C. C., Sarneel, J. M., Scharnweber, T., Schmeddes, J., Schmidt, M., Scholten, T., Schuchardt, M., Schwartz, N., Scott, T., Seeber, J., Segalin de Andrade, A. C., Seipel, T., Semenchuk, P., Senior, R. A., Serra-Diaz, J. M., Sewerniak, P., Shekhar, A., Sidenko, N. V., Siebicke, L., Siegwart Collier, L., Simpson, E., Siqueira, D. P., Sitková, Z., Six, J., Smiljanic, M., Smith, S. W., Smith-Tripp, S., Somers, B., Sørensen, M. V., Souza, J. J. L. L., Souza, B. I., Souza Dias, A., Spasojevic, M. J., Speed, J. D. M., Spicher, F., Stanisci, A., Steinbauer, K., Steinbrecher, R., Steinwandter, M., and Stemkov, M.: Global maps of soil temperature, Global Change Biol., 28, 3110–3144, https://doi.org/10.1111/gcb.16060, 2022.

Lindroth, A., Lagergren, F., Aurela, M., Bjarnadottir, B., Christensen, T., Dellwik, E., Grelle, A., Ibrom, A., Johansson, T., Lankreijer, H., Launiainen, S., Laurila, T., Mölder, M., Nikinmaa, E., Pilegaard, K., Sigurdsson, B. D., and Vesala, T.: Leaf area index is the principal scaling parameter for both gross photosynthesis and ecosystem respiration of Northern deciduous and coniferous forests, Tellus B, 60, 129–142, 2008.

Lin, S., Li, J., Liu, Q., Gioli, B., Paul-Limoges, E., Buchmann, N., Gharun, M., Hörtnagl, L., Foltýnová, L., Dušek, J., Li, L., and Yuan, W.: Improved global estimations of gross primary productivity of natural vegetation types by incorporating plant functional type, Int. J. Appl. Earth Obs. Geoinf., 100, 102328, https://doi.org/10.1016/j.jag.2021.102328, 2021.

Liu, Y.: Optimum temperature for photosynthesis: from leaf- to ecosystem-scale, Sci. Bull., 65, 601–604, https://doi.org/10.1016/j.scib.2020.01.006, 2020.

Liu, Y., Hansen, B. U., Elberling, B., and Westergaard-Nielsen, A.: Snow depth and the associated offset in ground temperatures in a landscape manipulated with snow-fences, Geoderma, 438, 116632, https://doi.org/10.1016/j.geoderma.2023.116632, 2023.

Lloyd, J. and Taylor, J. A.: On the temperature dependence of soil respiration, Funct. Ecol., 8, 315–323, 1994.

Lozano-Parra, J., Pulido, M., Lozano-Fondón, C., and Schnabel, S.: How do soil moisture and vegetation covers influence soil temperature in drylands of Mediterranean regions?, Water, 10, 1747, https://doi.org/10.3390/w10121747, 2018.

McNally, A., Arsenault, K., Kumar, S., Shukla, S., Peterson, P., Wang, S., Funk, C., Peters-Lidard, C. D., and Verdin, J. P.: A land data assimilation system for sub-Saharan Africa food and water security applications, Sci. Data 4, 170012, https://doi.org/10.1038/sdata.2017.12, 2017.

Migliavacca, M., Reichstein, M., Richardson, A. D., Colombo, R., Sutton, M. A., Lasslop, G., Tomelleri, E., Wohlfahrt, G., Carvalhais, N., Cescatti, A., Mahecha, M. D., Montagnani, L., Papale, D., Zaehle, S., Arain, A., Arneth, A., Black, T. A., Carrara, A., Dore, S., Gianelle, D., Helfter, C., Hollinger, D., Kutsch, W. L., Lafleur, P. M., Nouvellon, Y., Rebmann, C., Da Rocha, H. R., Rodeghiero, M., Roupsard, O., Sebastià, M.-T., Seufert, G., Soussana, J.-F., and Van Der Molen, M. K.: Semiempirical modeling of abiotic and biotic factors controlling ecosystem respiration across eddy covariance sites, Glob. Change Biol., 17, 390–409, https://doi.org/10.1111/j.1365-2486.2010.02243.x, 2011.

Myneni, R. B., Keeling, C. D., Tucker, C. J., Asrar, G., and Nemani, R. R.: Increased plant growth in the northern high latitudes from 1981 to 1991, Nature 386, 698–702, https://doi.org/10.1038/386698a0, 1997.

Niu, S., Luo, Y., Fei, S., Montagnani, L., Bohrer, G., Janssens, I. A., Gielen, B., Rambal, S., Moors, E., and Matteucci, G.: Seasonal hysteresis of net ecosystem exchange in response to temperature change: patterns and causes, Global Change Biol., 17, 3102–3114, 2011.

Nørgaard Nielsen, C. C. and Rasmussen, H. N.: Frost hardening and dehardening in Abies procera and other conifers under differing temperature regimes and warm-spell treatments, Forestry, 82, 43–59, https://doi.org/10.1093/forestry/cpn048, 2008.

Notarnicola, C.: Overall negative trends for snow cover extent and duration in global mountain regions over 1982–2020, Sci. Rep., 12, 13731, https://doi.org/10.1038/s41598-022-16743-w, 2022.

Nyberg, M. and Hovenden, M. J.: Warming increases soil respiration in a carbon-rich soil without changing microbial respiratory potential, Biogeosciences, 17, 4405–4420. https://doi.org/10.5194/bg-17-4405-2020, 2020.

Öquist, G. and Huner, N. P. A.: Photosynthesis of overwintering evergreen plants, Annu. Rev. Plant Biol., 54, 329–355, https://doi.org/10.1146/annurev.arplant.54.072402.115741, 2003.

Oddi, L., Migliavacca, M., Cremonese, E., Filippa, G., Vacchiano, G., Siniscalco, C., Morra di Cella, U., and Galvagno, M.: Contrasting responses of forest growth and carbon sequestration to heat and drought in the Alps, Environ. Res. Lett., 17, 045015, https://doi.org/10.1088/1748-9326/ac5b3a, 2022.

Pastorello, G., Trotta, C., Canfora, E., Chu, H., Christianson, D., Cheah, Y.-W., Poindexter, C., Chen, J., Elbashandy, A., Humphrey, M., Isaac, P., Polidori, D., Reichstein, M., Ribeca, A., van Ingen, C., Vuichard, N., Zhang, L., Amiro, B., Ammann, C., Arain, M. A., Ardö, J., Arkebauer, T., Arndt, S. K., Arriga, N., Aubinet, M., Aurela, M., Baldocchi, D., Barr, A., Beamesderfer, E., Belelli Marchesini, L., Bergeron, O., Beringer, J., Bernhofer, C., Berveiller, D., Billesbach, D., Black, T. A., Blanken, P. D., Bohrer, G., Boike, J., Bolstad, P. V., Bonal, D., Bonnefond, J.-M., Bowling, D. R., Bracho, R., Brodeur, J., Brümmer, C., Buchmann, N., Burban, B., Burns, S. P., Buysse, P., Cale, P., Cavagna, M., Cellier, P., Chen, S., Chini, I., Christensen, T. R., Cleverly, J., Collalti, A., Consalvo, C., Cook, B. D., Cook, D., Coursolle, C., Cremonese, E., Curtis, P. S., D'Andrea, E., da Rocha, H. R., Dai, X., Davis, K. J., De Cinti, B., de Grandcourt, A., De Ligne, A., De Oliveira, R. C., Delpierre, N., Desai, A. R., Di Bella, C. M., di Tommasi, P., Dolman, H., Domingo, F., Dong, G., Dore, S., Duce, P., Dufrêne, E., Dunn, A., Dušek, J., Eamus, D., Eichelmann, U., ElKhidir, H. A. M., Eugster, W., Ewenz, C. M., Ewers, B., Famulari, D., Fares, S., Feigenwinter, I., Feitz, A., Fensholt, R., Filippa, G., Fischer, M., Frank, J., Galvagno, M., Gharun, M., Gianelle, D., Gielen, B., Gioli, B., Gitelson, A., Goded, I., Goeckede, M., Goldstein, A. H., Gough, C. M., Goulden, M. L., Graf, A., Griebel, A., Gruening, C., Grünwald, T., Hammerle, A., Han, S., Han, X., Hansen, B. U., Hanson, C., Hatakka, J., He, Y., Hehn, M., Heinesch, B., Hinko-Najera, N., Hörtnagl, L., Hutley, L., Ibrom, A., Ikawa, H., Jackowicz-Korczynski, M., Janouš, D., Jans, W., Jassal, R., Jiang, S., Kato, T., Khomik, M., Klatt, J., Knohl, A., Knox, S., Kobayashi, H., Koerber, G., Kolle, O., Kosugi, Y., Kotani, A., Kowalski, A., Kruijt, B., Kurbatova, J., Kutsch, W. L., Kwon, H., Launiainen, S., Laurila, T., Law, B., Leuning, R., Li, Y., Liddell, M., Limousin, J.-M., Lion, M., Liska, A. J., Lohila, A., López-Ballesteros, A., López-Blanco, E., Loubet, B., Loustau, D., Lucas-Moffat, A., Lüers, J., Ma, S., Macfarlane, C., Magliulo, V., Maier, R., Mammarella, I., Manca, G., Marcolla, B., Margolis, H. A., Marras, S., Massman, W., Mastepanov, M., Matamala, R., Matthes, J. H., Mazzenga, F., McCaughey, H., McHugh, I., McMillan, A. M. S., Merbold, L., Meyer, W., Meyers, T., Miller, S. D., Minerbi, S., Moderow, U., Monson, R. K., Montagnani, L., Moore, C. E., Moors, E., Moreaux, V., Moureaux, C., Munger, J. W., Nakai, T., Neirynck, J., Nesic, Z., Nicolini, G., Noormets, A., Northwood, M., Nosetto, M., Nouvellon, Y., Novick, K., Oechel, W., Olesen, J. E., Ourcival, J.-M., Papuga, S. A., Parmentier, F.-J., Paul-Limoges, E., Pavelka, M., Peichl, M., Pendall, E., Phillips, R. P., Pilegaard, K., Pirk, N., Posse, G., Powell, T., Prasse, H., Prober, S. M., Rambal, S., Rannik, Ü., Raz-Yaseef, N., Rebmann, C., Reed, D., Resco de Dios, V., Restrepo-Coupe, N., Reverter, B. R., Roland, M., Sabbatini, S., Sachs, T., Saleska, S. R., Sánchez-Cañete, E. P., Sanchez-Mejia, Z. M., Schmid, H. P., Schmidt, M., Schneider, K., Schrader, F., Schroder, I., Scott, R. L., Sedlák, P., Serrano-Ortíz, P., Shao, C., Shi, P., Shironya, I., Siebicke, L., Šigut, L., Silberstein, R., Sirca, C., Spano, D., Steinbrecher, R., Stevens, R. M., Sturtevant, C., Suyker, A., Tagesson, T., Takanashi, S., Tang, Y., Tapper, N., Thom, J., Tomassucci, M., Tuovinen, J.-P., Urbanski, S., Valentini, R., van der Molen, M., van Gorsel, E., van Huissteden, K., Varlagin, A., Verfaillie, J., Vesala, T., Vincke, C., Vitale, D., Vygodskaya, N., Walker, J. P., Walter-Shea, E., Wang, H., Weber, R., Westermann, S., Wille, C., Wofsy, S., Wohlfahrt, G., Wolf, S., Woodgate, W., Li, Y., Zampedri, R., Zhang, J., Zhou, G., Zona, D., Agarwal, D., Biraud, S., Torn, M., and Papale, D.: The FLUXNET2015 dataset and the ONEFlux processing pipeline for eddy covariance data, Sci. Data, 7, 225, https://doi.org/10.1038/s41597-020-0534-3, 2020.

Randerson, J. T., Field, C. B., Fung, I. Y., and Tans, P. P.: Increases in early season ecosystem uptake explain recent changes in the seasonal cycle of atmospheric CO_2 at high northern latitudes, Geophys. Res. Lett., 26, 2765–2768, https://doi.org/10.1029/1999GL900500, 1999.

Reichstein, M., Tenhunen, J. D., Roupsard, O., Ourcival, J.-M., Rambal, S., Dore, S., and Valentini, R.: Ecosystem respiration in two Mediterranean evergreen holm oak forests: drought effects and decomposition dynamics, Funct. Ecol., 16, 27–39, https://doi.org/10.1046/j.0269-8463.2001.00597.x, 2002.

Repo, T., Domisch, T., Kilpeläinen, J., and Mäkinen, H.: Soil frost affects stem diameter growth of Norway spruce with delay, Trees, 35, 761–767, https://doi.org/10.1007/s00468-020-02074-8, 2021.

Running, S. W., Nemani, R. R., Heinsch, F. A., Zhao, M., Reeves, M., and Hashimoto, H.: A continuous satellite-derived measure of global terrestrial primary production, BioScience, 54, 547–560, https://doi.org/10.1641/0006-3568(2004)054[0547:ACSMOG]2.0.CO;2, 2004.

Shekhar, A., Hörtnagl, L., Buchmann, N., and Gharun, M.: Long-term changes in forest response to extreme atmospheric dryness, Glob. Change Biol., 29, 5379–5396, https://doi.org/10.1111/gcb.16846, 2023.

Shekhar, A., Hörtnagl, L., Paul-Limoges, E., Etzold, S., Zweifel, R., Buchmann, N., and Gharun, M.: Contrasting impact of extreme soil and atmospheric dryness on the functioning of trees and forests, Sci. Total Enviro., 916, 169931, https://doi.org/10.1016/j.scitotenv.2024.169931, 2024.

Sperling, O., Earles, J. M., Secchi, F., Godfrey, J., and Zwieniecki, M. A.: Frost induces respiration and accelerates carbon depletion in trees, PLoS ONE, 10, e0144124, https://doi.org/10.1371/journal.pone.0144124, 2015.

Strimbeck, G. R. and Schaberg, P. G.: Going to extremes: low temperature tolerance and acclimation in temperate and boreal conifers, in: Plant cold hardiness: from the laboratory to the field, edited by: Gusta, L., Wisniewski, M., and Tanino, K., 226–239, Wallingford, Oxfordshire, UK, CABI Publishing, ISBN-13: 978-1-84593-513-9, 2009.

Sullivan, P. F., Stokes, M. C., McMillan, C. K., and Weintraub, M. N.: Labile carbon limits late winter microbial activity near Arctic treeline, Nat. Commun., 11, 4024, https://doi.org/10.1038/s41467-020-17790-5, 2020.

Thurner, M., Beer, C., Santoro, M., Carvalhais, N., Wutzler, T., Schepaschenko, D., Shvidenko, A., Kompter, E., Ahrens, B., Levick, S. R., and Schmullius, C.: Carbon stock and density of northern boreal and temperate forests, Glob. Change Biol., 23, 297–310, https://doi.org/10.1111/geb.12125, 2014.

Tian, J., Zong, N., Hartley, I. P., He, N., Zhang, J., Powlson, D., Zhou, J., Kuzyakov, Y., Zhang, F., Yu, G., and Dungait, J. A. J.: Microbial metabolic response to winter warming stabilizes soil carbon, Glob. Change Biol., 27, 2011–2028, https://doi.org/10.1111/gcb.15538, 2021.

Tixier, A., Guzmán-Delgado, P., Sperling, O., Amico Roxas, A., Laca, E., and Zwieniecki, M. A.: Comparison of phenological traits, growth patterns, and seasonal dynamics of non-structural carbohydrate in Mediterranean tree crop species, Sci. Rep., 10, 347, https://doi.org/10.1038/s41598-019-57016-3, 2020.

Troeng, E. and Linder, S.: Gas exchange in a 20-year-old stand of Scots pine, 1. Net photosynthesis of current and one-year-old shoots within and between seasons, Physiol. Plant., 54, 15–23, 1982.

Warm Winter 2020 Team and ICOS Ecosystem Thematic Centre: Warm Winter 2020 ecosystem eddy covariance flux product for 73 stations in FLUXNET-Archive format – release 2022-1 (Version 1.0), ICOS Carbon Portal [data set], https://doi.org/10.18160/2G60-ZHAK, 2022.

Wang, Y., Liu, H., Chung, H., Yu, L., Mi, Z., Geng, Y., Jing, X., Wang, S., Zeng, H., Cao, G., Zhao, X., and He, J.-S.: Non-growing-season soil respiration is controlled by freezing and thawing processes in the summer monsoon-dominated Tibetan alpine grassland, Global Biogeochem. Cy., 28, 1081–1095, https://doi.org/10.1002/2013GB004760, 2014.

Weng, J.-H. and Liao, T.-S.: Photosynthetic responses and acclimation to temperature in seven conifers grown from low to high elevations in subtropical Taiwan, Taiwan J. Forest Sci., 25, 117–127, 2010.

Woods, S. W., Ahl, R., Sappington, J., and McCaughey, W.: Snow accumulation in thinned lodgepole pine stands, Montana, USA, Forest Ecol. Manag., 235, 202–211, https://doi.org/10.1016/j.foreco.2006.08.013, 2006.

Zhu, W. Z., Xiang, J. S., Wang, S. G., and Li, M. H.: Resprouting ability and mobile carbohydrate reserves in an oak shrubland decline with increasing elevation on the eastern edge of the Qinghai-Tibet Plateau, Forest Ecol. Manag., 278, 118–126, 2012.